

Pariser-Parr-Pople Model based Investigation of Ground and Low-Lying Excited States of Long Acenes

Himanshu Chakraborty and Alok Shukla*

Department of Physics, Indian Institute of Technology Bombay, Powai, Mumbai 400076, INDIA

E-mail: chakraborty.himanshu@gmail.com, shukla@phy.iitb.ac.in

*To whom correspondence should be addressed

Abstract

Several years back Angliker *et al.* [Chem. Phys. Lett. **1982**, 87, 208] predicted nonacene to be the first linear acene with the triplet state 1^3B_{2u} as the ground state, instead of the singlet 1^1A_g state. However, contrary to that prediction, in a recent experimental work Tönshoff and Bettinger [Angew. Chem. Int. Ed. **2010**, 49, 4125] demonstrated that nonacene has a singlet ground state. Motivated by this experimental finding, we decided to perform a systematic theoretical investigation of the nature of the ground, and the low-lying excited states of long acenes, with an emphasis on the singlet-triplet gap, starting from naphthalene, all the way up to decacene. Methodology adopted in our work is based upon Pariser-Parr-Pople model (PPP) Hamiltonian, along with large-scale multi-reference singles-doubles configuration interaction (MRSDCI) approach. Our results predict that even though the singlet-triplet gap decreases with the increasing conjugation length, nevertheless, it remains finite till decacene, thus providing no evidence of the predicted singlet-triplet crossover. We also analyze the nature of many-particle wavefunction of the correlated singlet ground state and find that the longer acenes exhibit tendency towards a open-shell singlet ground state. Moreover, when we compare the experimental absorption spectra of octacene and nonacene with their calculated singlet and triplet absorption spectra, we observe excellent agreement for the singlet case. Hence, the optical absorption results also confirm the singlet nature of the ground state for longer acenes. Calculated triplet absorption spectra of acenes predict two well separated intense long-axis polarized absorptions, as against one such peak observed for the singlet case. This is an important prediction regarding the triplet optics of acenes, which can be tested in future experiments on oriented samples.

Keywords: oligoacenes, octacene, nonacene, optical absorption spectrum, singlet-triplet gap, PPP model Hamiltonian, configuration-interaction method.

Introduction

Polyacenes, which can be seen as linearly fused benzene rings, are known for their well defined structures, and crystalline forms.¹⁻⁶ Because of their small band gaps and high charge-carrier mobilities, they find potential applications in novel opto-electronic devices such as light-emitting diodes, and field effect transistors *etc.*, which make them experimentally and theoretically a very important class of materials.^{7,8} In spite of a long tradition of research,⁹ the field of acenes has experienced a resurgence of interest in recent years because they are also perceived as the building blocks for organic electronic materials such as graphene nanoribbons.^{7,10}

Although pentacene, has excellent optical and transport properties, however, it is conceivable that the longer acenes could have even more attractive properties, with possible applications in the field of nanotechnology.¹⁰ As the size of the longer acenes approaches the nanometer scale, their reactivity also increases, and, therefore, it has been difficult to synthesize them from heptacene onwards.¹¹ Recently, many efforts have been made to synthesize the longer acenes, *e.g.*, heptacene and its functionalized derivatives have been synthesized by several workers.¹²⁻¹⁶ By using cryogenic matrix-isolation technique, and a protection group strategy, octacene and nonacene have been synthesized by Tönshoff and Bettinger¹⁷, while Kaur *et al.*¹⁸ prepared functionalized nonacene.

While all the known oligoacenes ranging from naphthalene to hexacene have a singlet ground state, some years back Angliker *et al.*¹⁹ predicted nonacene to be the first linear acene with the triplet state (1^3B_{2u}) as the ground state, instead of the singlet one (1^1A_g). Their prediction was based upon: (a) an extrapolation of the available experimental values of the singlet-triplet gap of the shorter acenes, and (b) theoretical calculations of the triplet states (1^3B_{2u}) of acenes using the singles configuration interaction (SCI) method, and the Pariser-Parr-Pople (PPP) model Hamiltonian.¹⁹ This was an interesting prediction because, if true, it could open the possibilities of magnetic applications of longer acenes. The singlet-triplet crossover in long acenes, predicted in this early work of Angliker *et al.*¹⁹, was also verified by Houk *et al.*²⁰ based upon first-principles density-functional-theory (DFT) based calculations. However, subsequent theoretical

investigations have predicted long acenes to have singlet ground states. They include PPP model based density-matrix renormalization group (DMRG) calculations of Raghu *et al.*,²¹, valence-bond theory based work of Gao *et al.*,²² first-principles DFT calculations of Bendikov *et al.*,²³ *ab initio* DMRG calculations of Hachmann *et al.*,²⁴ DFT-based work of Jiang and Dai,²⁵ and first-principles coupled-cluster calculations of Hajgato *et al.*²⁶ Recently, based upon optical absorption experiments, Tönshoff and Bettinger¹⁷ demonstrated that nonacene has a singlet ground state, thus contradicting the prediction of Angliker *et al.*¹⁹ empirically. Motivated by this experimental finding, we decided to perform a systematic theoretical investigation of the electronic structure of the ground and low-lying excited states of longer acenes, with an emphasis on the singlet-triplet gap, and their optical properties. In order to realize the possible potential of longer acenes in nanotechnology, a deep theoretical understanding of their electronic structure is very important. For our calculations, we adopt a methodology based upon the PPP model Hamiltonian, along with large-scale multi-reference singles-doubles configuration interaction (MRSDCI) approach.

First we benchmark our PPP-MRSDCI methodology by performing calculations of the singlet-triplet gaps of acenes ranging from naphthalene to decacene, and obtain results in very good quantitative agreement with those obtained by other wave-function-based approaches.^{21,24,26} Next, with the aim of understanding the experiments of Tönshoff and Bettinger,¹⁷ we compute the optical absorption spectra of octacene, nonacene, and decacene, both for the singlet and triplet manifolds. We discover that the results of our singlet optical absorption calculations are in excellent agreement with the experimental results for octacene and nonacene,¹⁷ leading us to conclude that the ground state in nonacene is of singlet multiplicity, against the predictions of Angliker *et al.*¹⁹ Although, the experimental results for decacene do not exist as of now, however, based upon the excellent quantitative agreement we obtain with the measured absorption spectra of octacene and nonacene, we predict that the ground state of decacene is also a singlet. Our computed optical absorption spectra for the triplet manifolds of octacene, nonacene, and decacene predict two major well-separated peaks polarized along the long axis, which can be tested in future experiments on longer acenes.

Theory

The schematic structures of higher polyacenes studied in this work are shown in Figure 1. The molecule is assumed to lie in the xy -plane, with the conjugation direction taken to be along the x -axis. The carbon-carbon bond length has been fixed at 1.4 \AA , and all bond angles have been taken to be 120° . It can be noted that these structures can also be seen as two polyene chains of suitable lengths, coupled together along the y -direction. The reason of choosing this symmetric geometry, against various other possibilities has already been discussed in our earlier paper.^{27,28} However, in the supporting information, we do consider an alternate geometry with nonuniform bond lengths,²³ and demonstrate that it leads to small quantitative changes in the optical absorption spectrum, compared to the results obtained using the uniform bond length. Thus, we conclude that small differences in the ground state geometry lead to insignificant changes in the optical absorption spectra of oligo acenes.

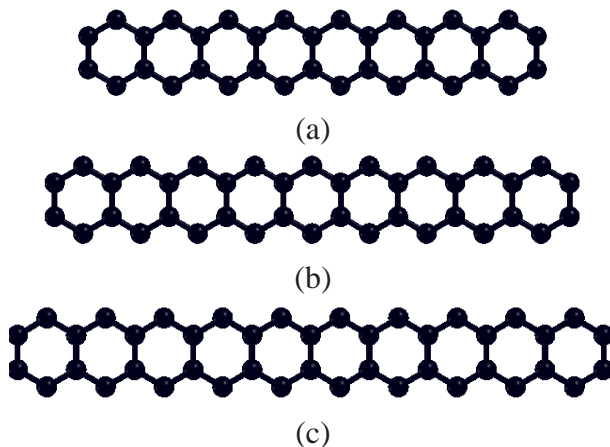


Figure 1: Schematic drawings of long acenes considered in this work, (a) octacene, (b) nonacene and (c) decacene. The x axis is assumed along the conjugation direction, while the y axis is perpendicular to it, in the plane of the figure.

The correlated calculations are performed using the PPP model Hamiltonian, which can be written as

$$H = H_{C_1} + H_{C_2} + H_{C_1C_2} + H_{ee},$$

where H_{C_1} and H_{C_2} are the one-electron Hamiltonians for the carbon atoms located on the upper and the lower polyene like chains, respectively. $H_{C_1C_2}$ is the one-electron hopping between the two chains, and H_{ee} depicts the electron-electron repulsion. The individual terms can now be written as,

$$H_{C_1} = -t_0 \sum_{\langle k, k' \rangle} B_{k, k'},$$

$$H_{C_2} = -t_0 \sum_{\langle \mu, \nu \rangle} B_{\mu, \nu},$$

$$H_{C_1C_2} = -t_{\perp} \sum_{\langle k, \mu \rangle} B_{k, \mu},$$

$$H_{ee} = U \sum_i n_{i\uparrow} n_{i\downarrow} + \frac{1}{2} \sum_{i \neq j} V_{i,j} (n_i - 1)(n_j - 1).$$

In the equation above, k, k' are carbon atoms on the upper polyene chain, μ, ν are carbon atoms located on the lower polyene chain, while i and j represent all the atoms of the oligomer. Symbol $\langle \dots \rangle$ implies nearest neighbors, and $B_{i,j} = \sum_{\sigma} (c_{i,\sigma}^{\dagger} c_{j,\sigma} + h.c.)$, where $c_{i,\sigma}^{\dagger}$ ($c_{i,\sigma}$) denotes the creation (annihilation) operator for a π orbital of spin σ , located on the i th carbon atom. Matrix elements t_0 , and t_{\perp} depict one-electron hops. As far as the values of the hopping matrix elements are concerned, we took $t_0 = 2.4$ eV for all nearest neighbor hopping with $t_{\perp} = t_0$, consistent with the undimerized ground state for polyacene argued by Raghu *et al.*²⁹

The Coulomb interactions are parametrized according to the Ohno relationship,³⁰

$$V_{i,j} = U / \kappa_{i,j} (1 + 0.6117 R_{i,j}^2)^{1/2},$$

where, $\kappa_{i,j}$ depicts the dielectric constant of the system which can simulate the effects of screening, U is the on-site repulsion term, and $R_{i,j}$ is the distance in Å between the i th and the j th carbon atoms. In the present work, we have performed calculations using “standard parameters”³⁰ with $U = 11.13$ eV and $\kappa_{i,j} = 1.0$, as well as “screened parameters”³¹ with $U = 8.0$ eV and $\kappa_{i,j} = 2.0$ ($i \neq j$) and $\kappa_{i,i} = 1.0$. The screened parameters employed here were devised by Chandross and Mazumdar³¹ with the aim of accounting for the inter chain screening effects in phenylene based polymers. However, in the present case, we compare our results of singlet and triplet absorption spectra of octacene and nonacene with the experimental spectra measured by Bettinger and co-workers,¹⁷ with the oligomers located inside the argon matrix. Therefore, here the purpose of screened parameters is to physically model the screening due to the argon matrix.

The starting point of the correlated calculations for the molecules is the Restricted Hartree-Fock (RHF) calculations, employing the PPP Hamiltonian, using a code developed in our group.³² All the resultant HF molecular orbitals are treated as active orbitals. The single-reference CI calculations such as the full/quadruple configuration interaction (FCI/QCI) were employed for shorter acenes, while the multi-reference singles doubles configuration interaction (MRSDCI) method was used for the longer ones. In particular, FCI method was used for naphthalene and anthracene, the QCI method was employed for the 1A_g and $^1B_{2u}$ symmetries of tetracene and pentacene, while for all other cases MRSDCI calculations were performed. The MRSDCI method is a well-established approach for including electron-correlation effects beyond the mean-field both for the ground and excited states of molecular systems.^{33,34} We have used this approach extensively within the PPP model to study the optical properties of a number of conjugated polymers,³⁵⁻³⁸ and it can be briefly summarized as follows. After the RHF calculations of the ground state 1^1A_g , the CI calculation of the ground state 1^1A_g , and the excited states of symmetries $^1B_{2u}$ and $^1B_{3u}$ are performed by taking the lowest energy configuration of the corresponding symmetry. They are $H \rightarrow L$ for B_{2u} and $H \rightarrow L + m$ and $H - m \rightarrow L$ ($m > 0$ is an integer whose value depends on the length of the oligomer) for B_{3u} , where H and L corresponds to Highest Occupied Molecular Orbital (HOMO) and Lowest Unoccupied Molecular Orbital (LUMO), respectively. A similar approach is adopted for the

triplet states as well, except that one has to ensure that the spin multiplicity of the wave functions is triplet. From the CI calculations, we obtain the eigenfunctions and eigenvalues corresponding to the correlated ground and excited states of the examined molecules. Using these eigenfunctions, the dipole matrix elements between the ground state and various excited states are computed. For the triplet states, the matrix elements are calculated with respect to the lowest triplet state 1^3B_{2u} . These dipole matrix elements, along with the energies of the excited states are, in turn, utilized to calculate linear (or triplet) optical absorption spectrum. Important excited states contributing to various peaks of the spectrum are identified, and a new set of MRSDCI calculations are performed with an increased number of reference configurations contributing both to the ground state, and the excited states, leading to a new absorption spectrum. This procedure is iterated until the computed spectrum converges satisfactorily.

Results and Discussions

In this section we present the results of our CI calculations on polyacenes ranging from naphthalene to decacene examining their singlet-triplet gaps, with the aim of determining the spin-multiplicity of their ground state. Furthermore, we also present MRSDCI calculations on the optical absorption of the long acenes, namely, octacene to decacene from their lowest triplet states (1^3B_{2u}), and the lowest-singlet state (1^1A_g), and compare the results with the experimental ones, where available.

Singlet-Triplet gap

We performed the first set of calculations to explore the singlet-triplet (1^1A_g - 1^3B_{2u}) gap in oligoacenes using the singles-configuration-interaction (SCI) method. The values of the singlet-triplet gap $\Delta E_{ST} = E(1^3B_{2u}) - E(1^1A_g)$ obtained from these calculations for oligoacenes up to acene-15 (acene- n denotes an oligomer with n benzene rings) are presented in Table 1. Examining the values of the singlet-triplet gap for various oligomers, it is obvious that: (a) in the standard-parameter based calculations, triplet state is never lower than the singlet one, while, (b) with the

screened parameters, the singlet and the triplet states become nearly degenerate for acene-7, and the crossover takes place starting with acene-8. In both sets of calculations, ΔE_{ST} first decreases with increasing n , and, subsequently begins to increase, suggesting the inadequacy of the SCI method for longer acenes. Nevertheless, our screened-parameter based SCI results appear to confirm the essential prediction of Angliker *et al.*¹⁹ that the singlet-triplet crossover will take place in oligoacenes with the increasing lengths, although, they differ in details in that Angliker *et al.*¹⁹ predicted the crossover from acene-9 onwards. Although Angliker *et al.*¹⁹ also used the PPP-SCI approach for their calculations, however, they used a smaller value of the nearest-neighbor hopping matrix element $t = -2.318$ eV, and a Mataga-Nishimoto³⁹ type Coulomb parameterization $V_{ij} = 1439.5/(132.8 + R_{ij})$, which corresponds to an effective value of $U = 10.84$ eV. It is obvious that the results of our SCI-PPP calculations differ from those of Angliker *et al.*¹⁹ because of different values of parameters employed. Furthermore, another calculation, performed by Houk *et al.*,²⁰ also predicted the singlet-triplet crossover in oligoacenes. However, *ab initio* DFT²⁰ can be unreliable for treating multi-reference correlation effects, which are important in the excited states of conjugated systems. Based upon past calculations performed on other polymers such as *trans*-polyacetylene,⁴⁰ it is a well-known fact that in order to be able to predict the correct excited state orderings in conjugated polymers, it is very important to account for the electron-correlation effects in an accurate manner. Therefore, we decided to go beyond the SCI approach, and performed large-scale CI calculations to explore the singlet-triplet ordering in polyacenes. Before we present and discuss our results, we would like to give a flavor to the reader as to the size of the CI calculations performed. Table 2 presents the number of reference states used in the MRSDCI calculations, and the total size of the resultant CI matrix. As mentioned in the previous section, the number of references (N_{ref}) used in various MRSDCI calculations was increased until acceptable convergence was achieved. For example, the convergence of the excitation energies of $1^1B_{2u}^+$ and $1^3B_{2u}^+$ states of nonacene with respect to N_{ref} , computed using the screened parameters, has been demonstrated explicitly in the Supporting Information.

The calculated values of the singlet-triplet gap are presented in Table 3, using both the standard

and the screened parameters, for the oligoacenes ranging from naphthalene to decacene. The variation of the calculated values of the singlet-triplet gap, and their comparison with the experimental and other theoretical calculations, for the oligoacenes ranging from naphthalene to decacene, as a function of the oligomer length, is presented in Figure 2. It is obvious both from the figure, that the excitation energy of 1^3B_{2u} state decreases as the oligomer length increases. Nevertheless, even for decacene the singlet-triplet gap is nonvanishing, and appears to saturate as a function of the increasing chain length. As far as comparison with the work of other authors is concerned, we observe the following trends in Figure 2: (a) Our standard parameter results are in good quantitative agreement with most other works, (b) in particular, our standard parameter results are in excellent agreement with the PPP-DMRG results of Raghu *et al.*,²¹ and also in very good agreement with the *ab initio* DMRG results of Hachmann *et al.*,²⁴ further vindicating our MRSDCI approach, and (c) our screened parameter results predict smaller values of the singlet-triplet gap as compared to other wave function based approaches for the shorter acenes, however, for longer ones they are also in good agreement with other results. However, DFT-based UB3LYP calculation performed by Bendikov *et al.*²³ agree with other works for shorter acenes, but for longer ones predict much smaller singlet-triplet gaps. We believe that these smaller gaps obtained in the work of Bendikov *et al.*,²³ could be attributed to the well-known tendency of DFT to underestimate the energy gaps. Therefore, based upon the fact that for decacene our calculations predict a singlet-triplet gap > 0.5 eV, we conclude that even for longer acenes, the singlet state 1^1A_g will be the ground state, and thus no singlet-triplet crossover of the kind predicted by Angliker *et al.*,¹⁹ occurs as per our calculations, and in agreement with all other works except that of Houk *et al.*²⁰ Recently, Hajgato *et al.*²⁶ performed first principles coupled cluster CCSD(T) calculations on the singlet-triplet gaps of acenes ranging from octacene to undecacene (acene-11), and their reported value of 0.58 eV for octacene is in almost perfect agreement with our PPP-MRSDCI results (*cf.* Table 3). However, for nonacene and decacene their reported values 0.46 eV and 0.35 eV²⁶, respectively, are smaller than both our standard and screened parameter values (*cf.* Table 3). Regarding the singlet-triplet gap in the polyacene limit ($n \rightarrow \infty$), DMRG-PPP work of Raghu *et al.*²¹ predicted it to be 0.53 eV, while

Gao *et al.*,²² using a spin Hamiltonian, estimated it to be 0.446 eV, both of which are reasonably close to our standard/screened parameters values of 0.57/0.54 eV, computed for decacene.

Bendikov *et al.*²³ noted that the restricted singlet density functional ground state of higher acenes would become unstable due to its open-shell nature, with two unpaired electrons (a singlet diradical⁴¹) for acenes longer than hexacene. Based upon *ab initio* DMRG calculations on acenes in the range $n = 2 - 12$, Hachmann *et al.*²⁴ concluded that the ground state wave functions for longer acenes were of the type of polyradical singlets. In another DFT work, Jiang and Dai²⁵ predicted the ground state of octacene and higher acenes to be antiferromagnetic (in other words, open-shell singlet), but not necessarily a diradical. Unlike the DFT calculations, in our approach, the many-body wave functions of the ground state and the excited states of the studied oligomers are available. Therefore, we decided to probe the nature of the ground state of longer acenes to ascertain whether, or not, they exhibit a polyradical character. The character of the many-body wave functions of the 1^1A_g ground state, obtained in our best CI calculations on oligomers ranging from naphthalene to decacene are presented in Table 4, for both the standard, and the screened parameters. From the results it is obvious that the singlet ground state of longer acenes begins to exhibit significant configuration mixing. With the increasing oligomer lengths, the contributions of several doubly-excited configurations to the ground state wave function increase. Thus, based upon these results, we conclude that the longer acenes studied in this work exhibit a tendency towards a singlet ground state, with a significant diradical open-shell character.

Table 1: The singlet-triplet gap ($\Delta E_{ST} = E(1^3B_{2u}) - E(1^1A_g)$) of acene- n , computed using the SCI method, and the standard (std), and the screened (scr) Coulomb parameters.

n	ΔE_{ST} (eV)	
	std	scr
2	2.66	2.07
3	1.63	1.16
4	1.04	0.63
5	0.68	0.32
6	0.42	0.12
7	0.34	0.00
8	0.26	-0.06
9	0.23	-0.10
10	0.24	-0.11
11	0.26	-0.12
15	0.41	-0.06

Table 2: The number of reference configurations (N_{ref}) and the total number of configurations (N_{total}) involved in the MRSDCI (or FCI or QCI, where indicated) calculations, for different symmetry subspaces of various oligoacenes.

n	$1A_g$		$1B_{2u}$		$3B_{2u}$	
	N_{ref}	N_{total}	N_{ref}	N_{total}	N_{ref}	N_{total}
2	1 ^a	4936 ^a	1 ^a	4794 ^a	1 ^a	4816 ^a
3	1 ^a	623576 ^a	1 ^a	618478 ^a	1 ^a	620928 ^a
4	1 ^b	193538 ^b	1 ^b	335325 ^b	100 ^c	323063 ^c
					86 ^d	319005 ^d
5	1 ^b	1002597 ^b	1 ^b	1707243 ^b	52 ^{c,d}	581702 ^{c,d}
6	100 ^c	1110147 ^c	100 ^c	1173212 ^c	65 ^c	1461526 ^c
	100 ^d	1177189 ^d	100 ^d	1328252 ^d	63 ^d	1551590 ^d
7	35 ^c	856788 ^c	30 ^c	674925 ^c	33 ^c	1369624 ^c
	22 ^d	615590 ^d	30 ^d	850627 ^d	29 ^d	1300948 ^d
8	18 ^c	768641 ^c	14 ^c	509119 ^c	19 ^c	1066355 ^c
	12 ^d	540651 ^d	4 ^d	145978 ^d	14 ^d	918645 ^d
9	13 ^c	959737 ^c	13 ^c	769387 ^c	18 ^c	1626229 ^c
	12 ^d	871397 ^d	3 ^d	186651 ^d	12 ^d	1152071 ^d
10	11 ^c	1202681 ^c	12 ^c	1192394 ^c	15 ^c	1735352 ^c
	11 ^d	1199887 ^d	3 ^d	270187 ^d	10 ^d	1318156 ^d

^aFCI method with standard as well as screened parameters,

^bQCI method with standard as well as screened parameters,

^cusing standard parameters,

^dusing screened parameters.

Table 3: For various oligomers, the singlet-triplet gaps ($\Delta E_{ST} = E(1^3B_{2u}) - E(1^1A_g)$) obtained from large-scale CI calculations (*cf.* Table 2), employing the PPP model Hamiltonian, and the standard (std) and screened (scr) parameters.

n	ΔE_{ST} (eV)	
	std	scr
2	2.53	2.11
3	1.73	1.48
4	1.25	1.11
5	0.99	0.93
6	0.87	0.85
7	0.73	0.69
8	0.68	0.58
9	0.60	0.56
10	0.57	0.54

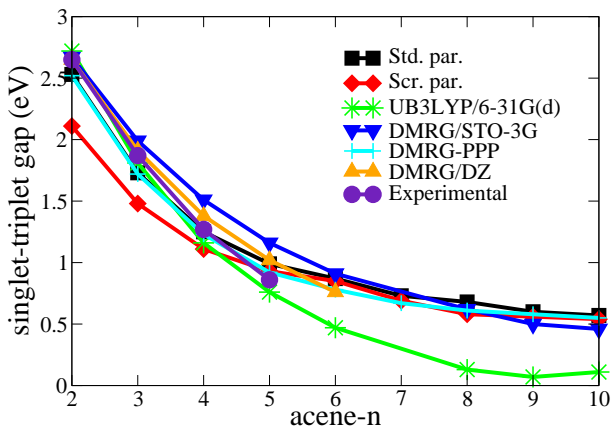


Figure 2: (Color online) Singlet-triplet energy gap as a function of the acene lengths.

Table 4: Magnitudes of the coefficients of the closed shell (CS) doubly excited virtual configuration $|H \rightarrow L; H \rightarrow L\rangle$, and the open shell (OS) doubly excited virtual configuration $|H \rightarrow L; H - 1 \rightarrow L + 1\rangle$ to the singlet 1^1A_g ground state CI wave functions of acene- n , obtained using the standard (std), and the screened (scr) parameters in the PPP model. In the preceding expression H stands for the highest occupied molecular orbital (HOMO), while L stands for lowest unoccupied molecular orbital (LUMO).

n	CS		OS	
	std	scr	std	scr
2	0.114	0.143	0.145	0.126
3	0.148	0.168	0.132	0.109
4	0.173	0.179	0.119	0.134
5	0.191	0.186	0.134	0.140
6	0.198	0.184	0.144	0.142
7	0.234	0.269	0.168	0.188
8	0.246	0.289	0.186	0.202
9	0.263	0.294	0.194	0.211
10	0.266	0.297	0.203	0.218

Singlet Linear Optical Absorption calculations

In an earlier work in our group, we had reported the calculations of linear optical absorption spectra of oligoacenes ranging from naphthalene to heptacene.²⁷ In this work, we extend our calculations to longer acenes, and present the calculations of linear optical absorption in octacene, nonacene and decacene. In Figures 4, 5 and 6, we present the singlet linear absorption spectra of these oligoacenes from their $1^1A_g^-$ singlet state computed using the standard parameters and the screened parameters. As per dipole selection rules for the D_{2h} symmetry, allowed one-photon transitions from the $1^1A_g^-$ state occur to $1^1B_{2u}^+$ ($1^1B_{3u}^+$) type states via short-axis (long-axis) polarized photons, where we assume that the short (long) axis correspond to y (x) directions. The essential states contributing to the linear absorption spectra of various acenes are depicted in Figure 3. The many-particle wave functions of the excited states contributing to various peaks in the spectra are presented in Tables 6-11 of the Supporting Information. While plotting the absorption spectra, we have restricted ourselves to states which lie below 6 eV, the estimated value of the ionization

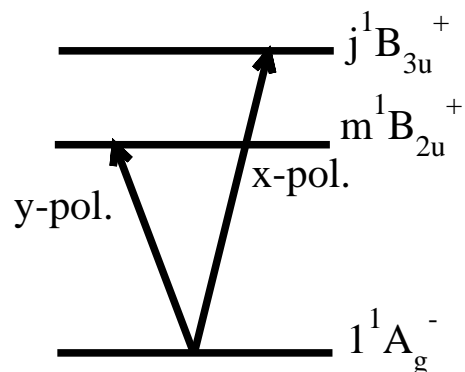


Figure 3: Diagram of the essential states involved in the singlet linear optical absorption in oligoacenes and their polarization characteristics. The arrows connecting two states imply optical absorption, with polarization directions stated next to them. Location of states is not up to scale.

A peak-by-peak detailed description of the computed singlet absorption spectra is provided in the Supporting Information. Here we list the salient features of the calculated linear optical absorption of octacene, nonacene, and decacene:

1. Quantitatively speaking, screened parameter spectra are redshifted as compared to the standard parameter ones.
2. Most of the intensity is concentrated in the x -polarized (long-axis polarized) spectra originating from the absorption into the $^1B_{3u}^+$ type of states, while the y -polarized (short-axis polarized) absorption into the $^1B_{2u}^+$ type states is comparatively weak. However, a closer examination reveals that most of the intensity in the x -polarized spectrum is derived from the single transition to an $n^1B_{3u}^+$ state (or states which split away from it). If we ignore this transition then the short- and long-axis polarized spectra are of comparable intensity. This aspect of the singlet linear absorption spectrum of long acenes is consistent with what is also observed in the shorter acenes.²⁷

3. The first peak corresponds to the y -polarized transition, to the $1^1B_{2u}^+$ excited state of the system. The most important configuration contributing to the many-particle wave function of the state corresponds to $|H \rightarrow L\rangle$ excitation, irrespective of the choice of the Coulomb parameters employed in the PPP model.
4. We have observed that the most intense absorption for the oligoacenes is through an x -polarized photon to a 1^1B_{3u} state, irrespective of the Coulomb parameters employed in the calculations. For acene- n , the many-particle wave function of this state exhibits the following general features: (a) for the standard parameter case, single excitations $|H \rightarrow L + n/2 - 1\rangle + c.c.$, for $n \equiv \text{even}$, and $|H \rightarrow L + (n - 1)/2\rangle + c.c.$, for $n \equiv \text{odd}$, dominate the wave function, while (b) with screened parameters the dominant configurations are single excitations $|H \rightarrow L + n/2\rangle + c.c.$ for $n \equiv \text{even}$, and $|H \rightarrow L + (n - 1)/2\rangle + c.c.$ for $n \equiv \text{odd}$. The aforesaid difference between the standard and the screened parameters is because of different energetic ordering of the symmetries of the molecular orbitals for the standard and screened parameters.

Figure 4: Singlet linear absorption spectra of octacene computed using: (a) standard parameters and (b) screened parameters. A uniform line width of 0.1 eV was assumed while plotting the spectra. The subscripts attached to the peak labels indicate the polarization directions x and y .

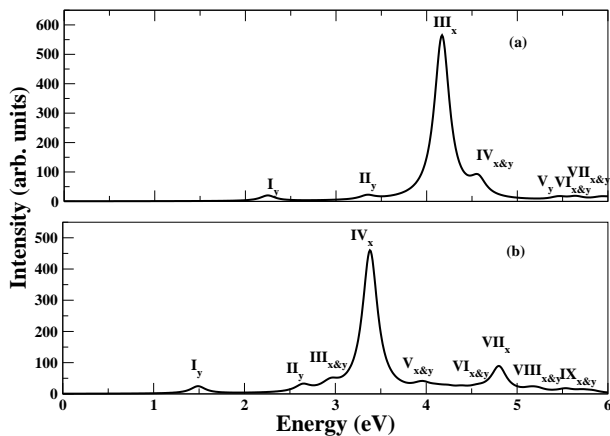


Figure 5: Singlet linear absorption spectra of nonacene computed using: (a) standard parameters and (b) screened parameters. The rest of the information is same as in the caption of Figure 4.

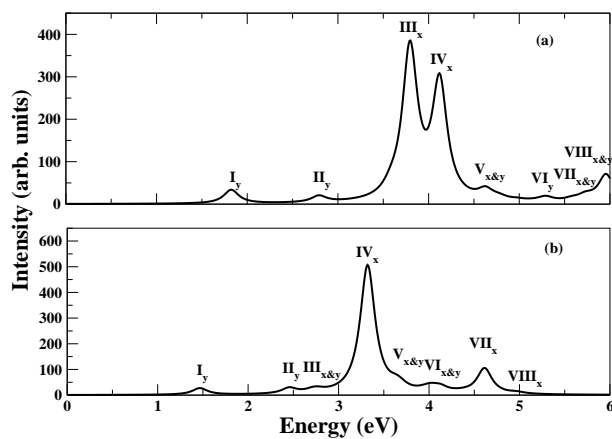
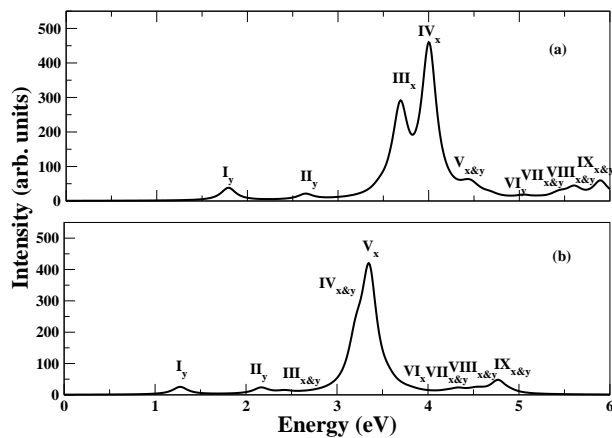


Figure 6: Singlet linear absorption spectra of decacene computed using: (a) standard parameters and (b) screened parameters. The rest of the information is same as in the caption of Figure 4.



Triplet optical absorption calculations

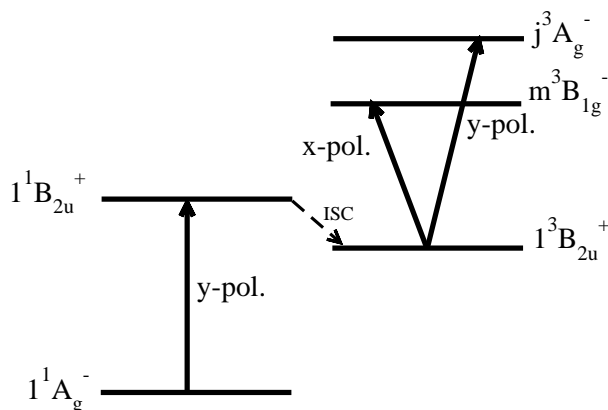


Figure 7: Diagram of the essential states involved in the triplet absorption spectra of oligoacenes, and their polarization characteristics. The arrows connecting two states imply optical absorption, with polarization directions stated next to them. Location of states is not up to scale. ISC refers to inter-system crossing.

In optical absorption experiments, one can probe the triplet excited states because frequently the first singlet excited state S_1 ($1^1B_{2u}^+$, in the present case) decays to the first triplet excited state T_1 ($1^3B_{2u}^+$, in the present case) located below S_1 , through nonradiative inter-system crossing (ISC), as shown in Figure 7. Once the system reaches the triplet manifold, normal optical absorption experiments can be performed to probe higher triplet states. In the present work, we restrict ourselves to the triplet one-photon absorption spectra of octacene, nonacene, and decacene from their $1^3B_{2u}^+$ state, computed using the MRSDCI method. For the case of oligoacenes, as per electric-dipole selection rules of the D_{2h} point group, the long-axis (x -axis) polarized photons cause transitions from the $1^3B_{2u}^+$ to $^3B_{1g}^-$ type of states, while the short-axis (y -axis) polarized ones lead to the $^3A_g^-$ type states (*cf.* Figure 7). The calculated triplet absorption spectra of these oligoacenes are displayed in Figures 8, 9 and 10, while the wave functions of the excited states contributing to various peaks in the spectra are presented in Tables 12-17 of the Supporting Information. While plotting the triplet absorption spectra, we have been careful to include only those states which lie below 6 eV excitation energy (with respect to the $1^1A_g^-$ state), which is the estimated value of the ionization

potentials of the long acenes.⁴² A detailed description of the characteristics of various peaks in the calculated triplet absorption spectra of octacene, nonacene, and decacene, is presented in the Supporting Information. Below we discuss the salient features of our results:

1. Similar to the case of singlet absorption, screened parameter spectra are red shifted as compared to the standard parameter ones.
2. Most of the intensity is concentrated in the x -polarized (long-axis polarized) spectra corresponding to the absorption into the ${}^3B_{1g}^-$ type of states, while the y -polarized absorption into the ${}^3A_g^-$ type states is very faint.
3. From Figures 8, 9, and 10 it is obvious that the triplet absorption spectrum is dominated by two intense x -polarized peaks which are well separated in energy (>2 eV), irrespective of the oligoacene in question, or the Coulomb parameters employed in the calculations. The first of these peaks is peak I in all the cases, while the second one is either peak IV or V, depending upon the oligoacene, or the Coulomb parameters employed. In the standard parameter based calculations, peak I is always the second most intense peak, while the second of these peaks (IV or V) is the most intense. In the screened parameter calculations the situation is exactly the reverse, with peak I being the most intense, while peak IV or V being the second most intense peak of the spectrum. Peak I always corresponds to the $1{}^3B_{1g}^-$ excited state of the system, whose wave function is dominated by the single excitations $|H \rightarrow L + 1\rangle + c.c.$, irrespective of the oligoacene in question, or the choice of Coulomb parameters. The second intense peak (IV or V) corresponds to a higher ${}^3B_{1g}^-$ type state of acene- n , whose wave function mainly consists of: (a) for the standard parameters, double excitations $|H \rightarrow L; H - (n/2 - 1) \rightarrow L\rangle + c.c.$ for $n \equiv \text{even}$, and $|H \rightarrow L; H - (n - 1)/2 \rightarrow L\rangle + c.c.$ for the $n \equiv \text{odd}$ case, while (b) for the screened parameters, double excitations $|H \rightarrow L; H - n/2 \rightarrow L\rangle + c.c.$ for $n \equiv \text{even}$, and $|H \rightarrow L; H - (n - 1)/2 \rightarrow L\rangle + c.c.$ for the $n \equiv \text{odd}$ case. This difference between the standard and the screened parameter results is because of the different energetic ordering of the molecular orbital symmetries in longer acenes, for the two sets of Coulomb

parameters.

- Other peaks in the spectrum correspond to either x or y polarized transitions to the higher excited states of the system, which are described in detail in the Supporting Information.

Figure 8: Triplet absorption spectra of octacene from the $1^3B_{2u}^+$ state computed using: (a) standard parameters and, (b) screened parameters. A uniform line width of 0.1 eV was assumed while plotting the spectra. The subscripts attached to the peak labels indicate the polarization directions x and y .

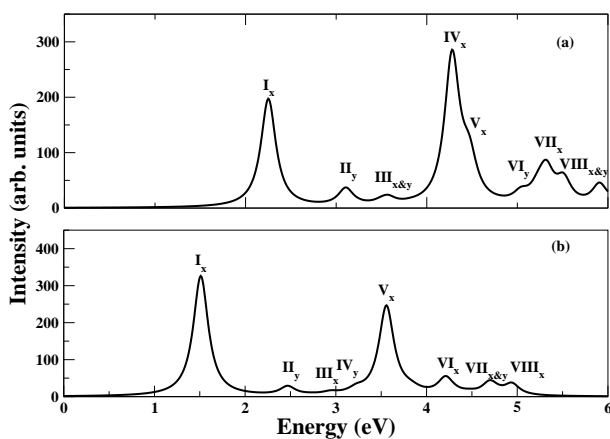


Figure 9: Triplet absorption spectra of nonacene from the $1^3B_{2u}^+$ state computed using: (a) standard parameters and, (b) screened parameters. The rest of the information is same as in the caption of Figure 8.

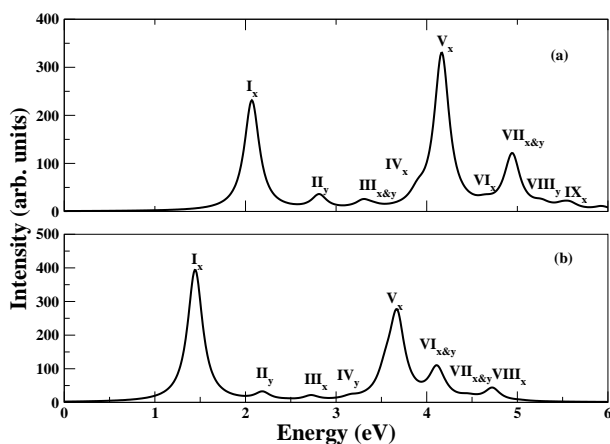
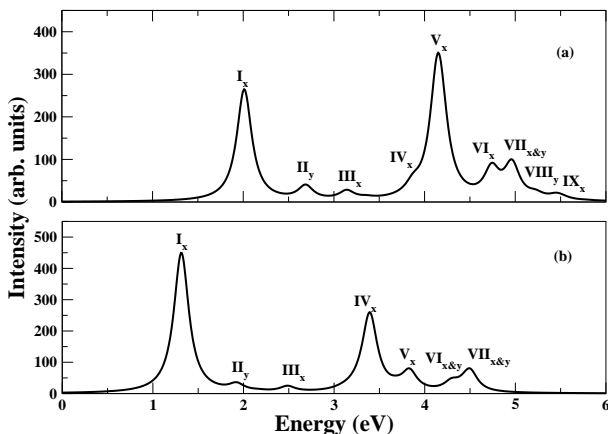


Figure 10: Triplet absorption spectra of decacene from the $1^3B_{2u}^+$ state computed using: (a) the standard parameters and, (b) the screened parameters. The rest of the information is same as in the caption of Figure 8.



Comparison of singlet and triplet absorption calculations of octacene and nonacene with the experimental results

In Table 5, the results of the experimental absorption of octacene and nonacene, reported by Tönshoff and Bettinger,¹⁷ have been presented, showing the excitation energies, relative intensities, and tentative assignments of the UV/vis electronic absorptions. Next, we compare our computed singlet and triplet absorption results, with the experimental ones, in terms of the peak energies (in eV) and relative intensities/oscillator strength. The relative oscillator strength (ROS) in the computed absorption spectra is the ratio of the calculated oscillator strength of a given state, with respect to that of the most intense state. The relative oscillator strengths of the peaks in the calculated absorption spectra are compared with the reported relative intensities (RI) of the corresponding peaks in the experimental spectra.

Octacene

On comparing the experimental values of the energies of the absorption peak of octacene from the Table 5a, with our calculated values for the singlet case (see Tables 6-7, Supporting Information), the lowest state S_1 (1.54 - 1.86 eV, RI = 0.025 for the 1.54 eV) of the experimental results matches nicely with the first peak at 1.49 eV (ROS = 0.050) obtained in the screened parameter calculations. We note that the first peak of our standard parameter calculations is located at 2.24 eV, and is thus significantly higher than the experimental value. The second state of the experimental results S_2 (2.40 eV, RI = 0.02) again agrees much better with the screened parameter result, 2.65 eV (ROS = 0.047) than with the standard parameter one located at 3.34 eV. The third state of the experimental results, S_3 (2.54 eV, RI = 0.050) has a better agreement with the third state of the screened parameter spectrum 2.97 eV (ROS = 0.046), than with corresponding standard parameter peak at 4.17 eV. The most intense peak in the experimental results corresponds to S_7 (3.68 - 3.78 eV, RI = 1.0) lies in between the highest peak of the screened and standard parameter calculations located at 3.38 eV (ROS = 1.0), and 4.17 eV (ROS = 1.0), respectively. We note that with the increasing peak energy, the agreement between the experiments and theory begins to deteriorate. Nevertheless, even in the worst case scenario of the most intense peak (S_7 of the experiments), the disagreement between the screened parameter results and the experiments is below 10%, as far as the peak location is concerned. This disagreement, which is fairly acceptable from a quantitative aspect, is possibly due to the reduced computational accuracy of our approach because of the high energies of the states involved. As far as the comparison of the experimental results with the triplet absorption calculations (see Tables 12-13, Supporting Information) is concerned, the first peaks in the computed triplet spectra, 3.04 eV (ROS = 0.839) for the standard parameter, and 1.97 eV (ROS = 1.0) for the screened parameters, disagree completely with the location of S_1 , as well as its relative intensity in the experimental spectrum. The same trend holds for the higher excited states as well. Thus, we conclude that the experimental absorption spectrum of octacene is indeed from the $1^1A_g^-$ ground state of the system, confirming yet again that the ground state of octacene has the singlet multiplicity.

We also note that Raghu *et al.*²¹ predicted a very large optical gap of 2.60 eV for octacene, based upon their DMRG calculations, employing the PPP Hamiltonian.

Nonacene

Similarly, comparing the experimental values of the energies of the absorption peak of nonacene from the Table 5b, with our calculated values for the singlet case (see Tables 8-9, Supporting Information), the lowest state S_1 (1.43 - 1.62 eV, RI = 0.020 for 1.43 eV) of the experimental results matches nicely with the first peak of 1.46 eV (ROS = 0.051) obtained in the screened parameter calculations, than the corresponding one for the standard parameter case located at 1.82 eV. The second state of the experimental results, S_3 (2.33 eV, RI = 0.033) again agrees much better with the second peak of the screened parameter result, 2.45 eV (ROS = 0.043) than with the standard parameter one located at 2.79 eV. The third state of the experimental results, S_4 (2.50 eV, RI = 0.023) has a better agreement with the third state of the screened parameter spectrum 2.71 eV (ROS = 0.020) than with the corresponding standard parameter peak at 3.80 eV. The most intense peak in the experimental results S_9 (3.66 eV, RI = 1.0) lies in between the highest peak of the screened and standard parameter calculations located at 3.32 eV (ROS = 1.0), and 3.80 eV (ROS = 1.0), respectively. For this most intense peak, the standard parameter results appear to agree slightly better with the experiments, as compared to the screened ones. But, keeping in mind the lower energy peaks discussed above, overall the screened parameter based results have a much better agreement with the experiments, just as in case of octacene. Similar to octacene, we again note that with the increasing peak energy, the agreement between the experiments and theory begins to deteriorate, which we again attribute to the reduced computational accuracy for higher energies. As far as the comparison of the experimental results with the triplet absorption calculations (see Tables 14-15, Supporting Information) is concerned, the first peaks in the computed triplet spectra, 2.56 eV (ROS = 0.785) for the standard parameter, and 1.86 eV (ROS = 1.0) for the screened parameters, disagree completely with the location of S_1 , as well as its relative intensity in the experimental spectrum. The same trend holds for the higher excited states as well. Thus, we conclude that the

experimental absorption spectrum of nonacene is indeed from the $1^1A_g^-$ ground state of the system, confirming yet again that the ground state of nonacene has the singlet multiplicity. Again, we note that the DMRG based calculations employing the PPP model, performed by Raghu *et al.*²¹ predict an unrealistically large optical gap of 2.59 eV for nonacene. Our values of the calculated optical gaps of octacene, nonacene, and decacene are in very good agreement with the estimated optical gap of polyacene 1.18 ± 0.06 eV, reported by Tönshoff and Bettinger.¹⁷

To conclude, the experimentalists are confident that the absorptions which they observed are all from the ground states of octacene and nonacene. Because, our singlet absorption spectra (as against the triplet absorption) computed using the screened parameters are in excellent agreement with those experiments, we conclude that the ground states of octacene and nonacene are of singlet multiplicity (1^1A_g), in perfect agreement with our singlet-triplet crossover calculations. Although the experiments have not been performed on acenes longer than nonacene, the trend emerging from our calculations leads us to conclude that the ground state will be of singlet type in those systems as well.

Table 5: The experimental values of the energies, relative intensities and tentative assignments of the UV/vis electronic absorptions of (a) octacene and (b) nonacene.¹⁷

(a)			(b)		
E(eV)	I (rel.)	Electronic State	E(eV)	I (rel.)	Electronic State
1.54	0.025	S_1	1.43	0.020	S_1
1.69	0.011		1.58	0.006	
1.73	0.016		1.62	0.016	
1.86	0.007		2.33	0.033	S_3
2.40	0.02	S_2	2.50	0.023	S_4
2.54	0.05	S_3	2.67	0.030	S_5
2.72	0.05		2.80	0.048	S_6
3.16	0.08	S_4	2.97	0.19	S_7
3.29	0.49	S_5	3.14	0.52	
3.33	0.43		3.42	0.14	S_8
3.48	0.46	S_6	3.66	1.00	S_9
3.68	0.90	S_7			
3.78	1.00				

Conclusions

To summarize, we presented large-scale MRSDCI calculations on the electronic structure and optical properties of oligoacenes, with focus on the longer acenes, namely, octacene, nonacene, and decacene. By performing such calculations on the lowest singlet and triplet states of oligomers ranging from naphthalene up to decacene, we established that the ground state in oligoacenes has singlet multiplicity, with a singlet-triplet gap of approximately 0.5 eV even for decacene. The trends visible from our calculations rule out a singlet-triplet crossover for the ground states of longer oligoacenes as well. This result of ours has thus resolved an old speculation predicting that nonacene onwards, the ground state of oligoacenes will be of triplet multiplicity.¹⁹

Moreover, the many-body wavefunction analysis of the correlated singlet ground state $1^1A_g^-$ reveals increasing contribution of configurations with two open shells, accompanied with the decreasing one from the closed-shell Hartree-Fock reference state, with the increasing chain length. Thus our calculations predict an open-shell diradical character for the singlet ground state of longer acenes.²³

As far as the singlet linear optical absorption is concerned, in all the acenes, the first peak is due to a y -polarized transition to the $1^1B_{2u}^+$ state, corresponding to the HOMO to LUMO transition. The most intense state is the x -polarized transition to a 1^1B_{3u} state, which is also dominated by single excitations. When we compare our singlet linear absorption spectra of octacene and nonacene with the experimental ones,¹⁷ excellent agreement is obtained on the important peak locations and intensity profiles. Furthermore, the measured absorption spectra of longer acenes show no resemblance with our computed triplet absorption spectra, confirming once again the conclusion that the ground state of the longer acenes is indeed singlet in nature.

Our calculations on the one-photon triplet absorption spectra predict two intense x -polarized absorptions, which are well separated in energy. Besides these two, there are a number of weaker peaks which are either x or y polarized. This is in sharp contrast to the singlet absorption which predicts only one intense peak. The existence of two well separated x -polarized peaks in the triplet absorption spectrum is one of the most important predictions of this work, and can be tested in

future experiments on oriented samples of longer acenes.

We also performed singlet and triplet optical absorption calculations on decacene, a molecule which has not been synthesized yet. We are hopeful that in future, once decacene is synthesized in the laboratory, our theoretical predictions could be tested in experiments.

In this paper we restricted ourselves to the low-lying excited states of longer acenes which contribute to their linear optical properties. However, not many calculations have been performed as far as the nonlinear optical properties of these materials are concerned. In particular, it will be of interest to compute the nonlinear susceptibilities corresponding to two-photon absorption, and third harmonic generation. Both these nonlinear optical processes have the capability to probe the higher excited states of polyacenes, which is essential in order to obtain a deeper understanding of the optical response of π electrons. At present, studies along these directions are underway in our group.

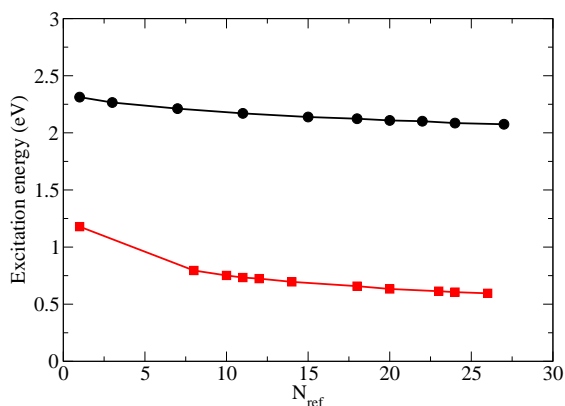
Acknowledgement

The authors thank Professor H. F. Bettinger (University of Tübingen) for communicating his experimental data before publications. One of us (H. C.) acknowledges the Council of Scientific and Industrial Research, (CSIR), India for the financial support (SRF award No. 20-06/2009(i)EU-IV).

Supporting Information Available

Convergence of Excitation Energies in MRSDCI Calculations

Figure 11: Behavior of 1^1B_{2u} (circles), 1^3B_{2u} (squares) excited states of nonacene with respect to the number of reference configurations (N_{ref}) included in the MRSDCI calculations performed using the screened parameters.



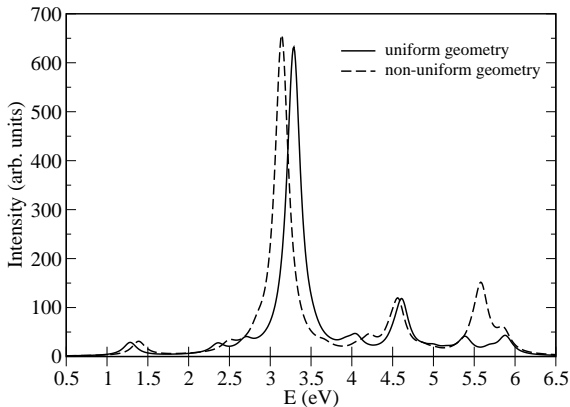
In order to demonstrate the convergence of our MRSDCI calculations, we present the plot of the excitation energies of two lowest states, singlet $1^1B_{2u}^+$ and triplet $1^3B_{2u}^+$, of nonacene, computed using the screened parameters, in Figure 11, calculated with increasing number of reference configurations (N_{ref}). It is obvious from the figure that the convergence has been achieved by the time twenty most important configurations ($N_{ref} = 20$) have been included in the calculations.

Influence of the Geometry on the Optical Absorption in Long Acenes

The issue of the ground state geometry in long acenes has been in debate for many years.^{21,23,24,26,29} Some theoretical calculations have predicted a symmetric ground state geometry to be lower,^{21,29} while others have indicated a highly non-uniform geometry to be the true ground state.^{23,24,26} In this work, consistent with the PPP model based work of Ramasesha and coworkers,^{21,29} and our

own work,^{27,28} we have used the symmetric ground state geometry for all oligoacenes, with all the C-C bonds equal to 1.4 Å, and all bond angles taken to be 120°. In order to investigate the influence of geometry on the optical absorption spectra, we performed calculations on nonacene using a highly non-uniform geometry reported for its closed-shell singlet ground state by Bendikov *et al.*,²³ obtained using the B3LYP exchange-correlation functional in DFT. As compared to the symmetric geometry, the nonuniformity is quite severe in this geometry, with the two polyene chains exhibiting bond alternation, and the interchain separation also varying significantly. The smallest C-C bond length in the nonuniform structure is ≈ 1.36 Å, while the largest one is close to 1.47 Å. For this nonuniform geometry, the hopping matrix elements between nearest-neighbor sites i and j , needed for the PPP calculations, were generated using the exponential formula $t_{ij} = t_0 e^{(r_0 - r_{ij})/\delta}$, where r_{ij} is the bond distance (in Å) between the sites, $t_0 = -2.4$ eV, $r_0 = 1.4$ Å, and the decay constant $\delta = 0.73$ Å. The value of δ was chosen so that the formula closely reproduces the hopping matrix elements for a bond-alternating polyene with short/long bonds 1.35/1.45 Å. The results of an SCI level calculation of the singlet optical absorption spectrum of nonacene, both for the uniform (symmetric) and this nonuniform geometry of Bendikov *et al.*,²³ computed using the screened parameters of the PPP model, are presented in Figure. 12. From the figure it is obvious that there are small quantitative differences between the two results, as far as peak locations are concerned. For example, the first peak (1^1B_{2u}) is slightly blueshifted (0.11 eV) for the nonuniform geometry, as compared to the symmetric geometry, while the most intense peak (1^1B_{3u}) is slightly redshifted (0.15 eV). The only qualitative change between the two results is at an energy higher than 5.5 eV, where one peak in the nonuniform geometry is more intense as compared to its neighboring peak. Therefore, we conclude that the variations in the ground state geometries of the magnitude considered here, lead to small quantitative, and insignificant qualitative, changes in the optical absorption spectra of oligoacenes.

Figure 12: Comparison of the calculated singlet optical absorption spectra for nonacene, with the uniform (symmetric) geometry, and the nonuniform geometry of Bendikov *et al.*,²³ computed at SCI level, employing the screened parameters in the PPP model.



Singlet linear absorption

In the following we present a detailed description of the calculated singlet linear absorption spectra of octacene, nonacene, and decacene, presented in Figures 4-6 of the main text for standard and the screened parameters.

1. For all the oligoacene, the first peak is due to a y -polarized transition, to the $1^1B_{2u}^+$ excited state of the system, whose wave function is dominated by the $|H \rightarrow L\rangle$ single excitation, irrespective of the choice of the Coulomb parameters employed in the PPP model.
2. The second peak also corresponds to a y -polarized transition, to the $2^1B_{2u}^+$ excited state of the system. The most important configuration contributing to the many-particle wave function of this state is $|H-1 \rightarrow L+1\rangle$ excitation, irrespective of the choice of the Coulomb parameters.
3. The nature of the third peak is dependent upon the Coulomb parameters employed in the PPP model. For the standard parameter case, this peak always corresponds to the x -polarized, $1^1B_{3u}^+$ excited state, signalling the onset of the most intense absorption feature in the system. For octacene, it is the single most intense peak, whose wave function mainly consists

of single excitations $|H \rightarrow L + 3\rangle + c.c.$ (*c.c.* denotes the charge conjugated configuration). For nonacene and decacene, perhaps due to band formation, it is the first of the two adjacent intense peaks which are x polarized. For nonacene it is the most intense peak, and the corresponding many-body wave function is dominated by the single excitation $|H \rightarrow L + 4\rangle + c.c.$. For decacene, however, it is the second most intense feature, and the double excitations $|H \rightarrow L; H \rightarrow L + 1\rangle + c.c.$ contribute the most to its many-body wave function.

In the screened parameter calculations, the third peak is a faint peak, containing a mixture of x and y polarized transition to the states, $1^1B_{3u}^+$ and $3^1B_{2u}^+$ of the system. For all the oligoacenes, the double excitation $|H \rightarrow L; H \rightarrow L + 1\rangle + c.c.$ contributes the most to the $1^1B_{3u}^+$ state, and the single excitation $|H \rightarrow L + 2\rangle + c.c.$ dominates the $3^1B_{2u}^+$ wave function.

4. For the standard parameter case, the fourth peak is a faint peak for octacene, consisting of a mixture of x - and y -polarized transitions to the states, $2^1B_{3u}^+$ and $4^1B_{2u}^+$. Double excitations $|H \rightarrow L; H \rightarrow L + 1\rangle + c.c.$ contribute the most to the $2^1B_{3u}^+$ state, and single excitations $|H - 2 \rightarrow L + 2\rangle + c.c.$ to the $4^1B_{2u}^+$ state. For nonacene and decacene, however, it is an intense x -polarized feature corresponding to the state $2^1B_{3u}^+$, which is adjacent to their $1^1B_{3u}^+$ state mentioned above. For the case of decacene, it also the most intense absorption of the system. Both for nonacene and decacene, the single excitations $|H \rightarrow L + 4\rangle + c.c.$ contribute the most to the many-particle wave function of this state.

For the screened parameter calculations, the fourth peak corresponds to the most intense absorption, through an x -polarized photon, to the $2^1B_{3u}^+$ state, in case of octacene and nonacene. For decacene, however, it appears as a shoulder to the most intense peak, consisting of a mixture of x and y polarized transitions, to the $2^1B_{3u}^+$ and $4^1B_{2u}^+$ states. The many-particle wave function of the $2^1B_{3u}^+$ state for octacene and nonacene is dominated by the single excitations $|H \rightarrow L + 4\rangle + c.c.$, while for decacene the double excitations $|H \rightarrow L + 1; H \rightarrow L + 2\rangle + c.c.$ dominate. The $4^1B_{2u}^+$ state of decacene has the maximum contribution from the single exci-

tation $|H - 2 \rightarrow L + 2\rangle$.

5. For the standard parameter case, the fifth peak is a very faint feature consisting of y -polarized transition to the state $7^1B_{2u}^+$ for octacene, whose wave function is dominated by the single excitation $|H - 2 \rightarrow L + 2\rangle$. However, for nonacene and decacene, it corresponds to the mixture of x and y polarized transitions to the states, $3^1B_{3u}^+$ and $5^1B_{2u}^+$, respectively. The double excitations $|H \rightarrow L + 1; H - 1 \rightarrow L + 1\rangle + c.c.$ for the $3^1B_{3u}^+$ state, and the triple excitation $|H \rightarrow L; H \rightarrow L; H - 1 \rightarrow L + 1\rangle$ for the $5^1B_{2u}^+$ state, contribute the most to their wave functions.

For the screened parameter case, it is a faint peak consisting of a mixture of x and y polarized transitions to the states, $3^1B_{3u}^+$ and $4^1B_{2u}^+$, respectively, for both octacene and nonacene. For decacene, however, it is the most intense peak corresponding to x polarized transition to the state $4^1B_{3u}^+$. The most important configuration contributing to the many-particle wave function of the state for octacene and nonacene, is a mixture of double excitations $|H \rightarrow L + 1; H \rightarrow L + 2\rangle + c.c.$ for $3^1B_{3u}^+$ state, and single excitations $|H - 2 \rightarrow L + 2\rangle$ for the $4^1B_{2u}^+$ state. For decacene, the single excitations $|H \rightarrow L + 5\rangle + c.c.$ contribute the most to the wavefunction of this state.

6. For the standard parameter case, the sixth peak corresponds to a mixture of x and y polarized transitions to the states, $4^1B_{3u}^+$ and $9^1B_{2u}^+$, respectively, for octacene. The many-body wave functions of both these states derive predominant contributions from double excitations: $|H \rightarrow L; H - 1 \rightarrow L + 2\rangle + c.c.$ for the $4^1B_{3u}^+$, and $|H \rightarrow L + 1; H \rightarrow L + 3\rangle + c.c.$ for the $9^1B_{2u}^+$ state. For nonacene (decacene), it corresponds to a y -polarized transition to the state $10^1B_{2u}^+$ ($9^1B_{2u}^+$), whose many-body wave function derives maximum contribution from the single excitation $|H - 2 \rightarrow L + 2\rangle$.

The same peak with the screened parameters is a mixture of x and y polarized transitions

for the case of octacene and nonacene. For octacene, transitions to states $6^1B_{3u}^+$ and $8^1B_{2u}^+$ constitute this peak, with double excitations $|H \rightarrow L; H \rightarrow L + 1\rangle + c.c.$ and $|H \rightarrow L; H \rightarrow L + 5\rangle + c.c.$, respectively, contributing most to their wave functions. For nonacene, this peak consists of three states $4^1B_{3u}^+$ and $6^1B_{2u}^+$ and $7^1B_{2u}^+$, with double excitation $|H \rightarrow L; H - 1 \rightarrow L + 2\rangle + c.c.$ contributing the most to the $4^1B_{3u}^+$, triple excitation $|H \rightarrow L; H \rightarrow L; H - 1 \rightarrow L + 1\rangle$ to the $6^1B_{2u}^+$, and the single excitation $|H - 2 \rightarrow L + 2\rangle$ to the $7^1B_{2u}^+$ state. However, for decacene, the peak is purely x polarized, due to transition to the state $6^1B_{3u}^+$ whose wave function derives maximum contribution from the double excitations $|H \rightarrow L; H \rightarrow L + 1\rangle + c.c.$.

7. The seventh peak in the standard parameter spectrum is both x and y polarized for all the three oligomers. For octacene, the peak involves $5^1B_{3u}^+$ and $10^1B_{2u}^+$ states, with single excitations $|H \rightarrow L + 7\rangle + c.c.$ and $|H - 2 \rightarrow L + 2\rangle$, respectively, contributing the most to their wave functions. For nonacene states $7^1B_{3u}^+$ and $12^1B_{2u}^+$ constitute the peak, with single excitation $|H \rightarrow L + 8\rangle + c.c.$ providing the maximum contribution to the $7^1B_{3u}^+$ state, and triple excitation $|H \rightarrow L; H - 1 \rightarrow L + 1; H - 1 \rightarrow L + 1\rangle$ to the $12^1B_{2u}^+$ state. For decacene, the peak involves $6^1B_{3u}^+$ and $11^1B_{2u}^+$ states, with double excitations $|H \rightarrow L; H - 1 \rightarrow L + 2\rangle + c.c.$ and triple excitations $|H \rightarrow L; H - 1 \rightarrow L + 1; H - 1 \rightarrow L + 1\rangle$, respectively, contributing the most to their wave functions.

With the screened parameters, the seventh peak of octacene and nonacene is x polarized, while for decacene it has mixed x and y polarizations. Both for octacene and nonacene states $8^1B_{3u}^+$ constitute this peak, with single excitation $|H - 1 \rightarrow L + 5\rangle + c.c.$ and $|H - 1 \rightarrow L + 6\rangle + c.c.$ providing main contributions to the wave functions of octacene, and nonacene, respectively. However, for decacene, transitions to states $8^1B_{3u}^+$ and $10^1B_{2u}^+$ form the peak, with double excitations $|H \rightarrow L; H - 1 \rightarrow L + 4\rangle + c.c.$ and single excitations $|H - 1 \rightarrow L + 7\rangle + c.c.$, respectively, contributing the most to their wave functions.

8. With the standard parameters, the eighth peak does not exist for octacene, while for nonacene

and decacene, it has mixed x and y polarizations. For nonacene, the states constituting the peak are $8^1B_{3u}^+$ and $16^1B_{2u}^+$, with single excitations $|H - 1 \rightarrow L + 5\rangle + c.c.$ and triple excitations $|H \rightarrow L; H \rightarrow L + 2; H - 1 \rightarrow L + 1\rangle + c.c.$, respectively, contributing to their wave functions. For decacene, three states $7^1B_{3u}^+$, $14^1B_{2u}^+$, and $15^1B_{2u}^+$, form this peak, with single excitations $|H \rightarrow L + 8\rangle + c.c.$, $|H \rightarrow L + 12\rangle + c.c.$, and $|H \rightarrow L + 9\rangle + c.c.$, respectively, contributing the most to their many-particle wave functions.

With the screened parameters case, the eighth peak is x and y polarized for octacene and decacene, while it is only x polarized for nonacene. For octacene, states $9^1B_{3u}^+$ and $13^1B_{2u}^+$ form this peak, whose wave functions, respectively, derive maximum contributions from single excitations $|H - 2 \rightarrow L + 4\rangle + c.c.$, and triple excitations $|H \rightarrow L; H - 1 \rightarrow L + 1; H - 1 \rightarrow L + 1\rangle$. In case of nonacene, the transition to the state $9^1B_{3u}^+$ leads to this peak, with single excitations $|H - 2 \rightarrow L + 4\rangle + c.c.$ contributing the most to its many-particle wave function. For decacene, states $9^1B_{3u}^+$ and $14^1B_{2u}^+$ constitute the peak, with the single excitations $|H \rightarrow L + 8\rangle + c.c.$ and $|H \rightarrow L + 9\rangle + c.c.$, respectively, providing the largest contributions to their wave functions.

9. The ninth peak, for the standard parameter case, exists only for decacene, and has a mixed x and y polarization, with states $8^1B_{3u}^+$ and $17^1B_{2u}^+$ forming the peak. The single excitations $|H - 2 \rightarrow L + 4\rangle + c.c.$ contribute the most to $8^1B_{3u}^+$ state, while double excitations $|H \rightarrow L; H - 1 \rightarrow L + 4\rangle + c.c.$ to the $17^1B_{2u}^+$ state.

With the screened parameters, the ninth peak does not exist for nonacene, and it is x and y polarized for octacene and decacene. For octacene, states $12^1B_{3u}^+$ and $16^1B_{2u}^+$ constitute this peak, with the double excitations $|H \rightarrow L; H - 1 \rightarrow L + 6\rangle + c.c.$ and single excitations $|H - 1 \rightarrow L + 7\rangle + c.c.$, respectively, contributing the most to their wave functions. For decacene, the states $11^1B_{3u}^+$ and $16^1B_{2u}^+$ form this peak, with the single excitations $|H - 2 \rightarrow L + 5\rangle + c.c.$ and $|H - 1 \rightarrow L + 7\rangle + c.c.$, respectively, providing the maximum

contributions to their wave functions.

Table 6: Excited states contributing to the singlet linear absorption spectrum of octacene computed using the MRSDCI method coupled with the standard parameters in the PPP model Hamiltonian. The table includes many-particle dominant contributing configurations, excitation energies, dipole matrix elements, and relative oscillator strengths (ROS) of various states with respect to the 1^1A_g ground state. DF corresponds to dipole forbidden state. Below, ‘+c.c.’ indicates that the coefficient of charge conjugate of a given configuration has the same sign, while ‘-c.c.’ implies that the two coefficients have opposite signs.

Peak	State	E (eV)	Transition Dipole (Å)	ROS	dominant contributing configurations
DF	$1^1B_{3u}^-$	2.31	0	0	$ H \rightarrow L; H \rightarrow L+1\rangle - c.c.(0.4948)$ $ H \rightarrow L; H-1 \rightarrow L+2\rangle - c.c.(0.1938)$
I	$1^1B_{2u}^+$	2.24	0.905	0.034	$ H \rightarrow L\rangle (-0.8471)$ $ H \rightarrow L; H \rightarrow L; H-1 \rightarrow L+1\rangle (0.0948)$
II	$2^1B_{2u}^+$	3.34	0.641	0.025	$ H-1 \rightarrow L+1\rangle (-0.5826)$ $ H \rightarrow L+2\rangle - c.c.(0.4284)$
III	$1^1B_{3u}^+$	4.17	3.622	1.000	$ H \rightarrow L+3\rangle + c.c.(0.4622)$ $ H \rightarrow L; H \rightarrow L+1\rangle + c.c.(0.2614)$
IV	$4^1B_{2u}^+$	4.51	0.367	0.011	$ H-2 \rightarrow L+2\rangle (-0.4148)$ $ H-1 \rightarrow L+4\rangle + c.c.(0.4020)$
	$2^1B_{3u}^+$	4.57	1.079	0.097	$ H \rightarrow L; H \rightarrow L+1\rangle + c.c.(0.3214)$ $ H \rightarrow L+3\rangle + c.c.(0.3214)$
V	$7^1B_{2u}^+$	5.46	0.375	0.014	$ H-2 \rightarrow L+2\rangle (0.3574)$ $ H \rightarrow L+6\rangle - c.c.(0.3489)$
VI	$9^1B_{2u}^+$	5.64	0.261	0.007	$ H \rightarrow L+1; H \rightarrow L+3\rangle + c.c.(0.3883)$ $ H \rightarrow L; H \rightarrow L+5\rangle + c.c.(0.2768)$
	$4^1B_{3u}^+$	5.65	0.335	0.012	$ H \rightarrow L; H-1 \rightarrow L+2\rangle - c.c.(0.4696)$ $ H \rightarrow L; H \rightarrow L+1\rangle + c.c.(0.1289)$
VII	$10^1B_{2u}^+$	5.89	0.203	0.004	$ H-2 \rightarrow L+2\rangle (-0.3657)$ $ H-3 \rightarrow L+3\rangle (0.3074)$
	$5^1B_{3u}^+$	5.94	0.307	0.010	$ H \rightarrow L+7\rangle - c.c.(0.3397)$ $ H \rightarrow L; H \rightarrow L+4\rangle + c.c.(0.2494)$

Table 7: Excited states contributing to the singlet linear absorption spectrum of octacene computed using the MRSDCI method coupled with the screened parameters in the PPP model Hamiltonian. The rest of the information is same as that in Table 6.

Peak	State	E (eV)	Transition Dipole (Å)	ROS	dominant contributing configurations
DF	$1^1B_{3u}^-$	1.59	0	0	$ H \rightarrow L; H \rightarrow L+1\rangle - c.c.(0.5078)$ $ H \rightarrow L; H-1 \rightarrow L+2\rangle - c.c.(0.1949)$
I	$1^1B_{2u}^+$	1.49	1.241	0.050	$ H \rightarrow L\rangle (0.8503)$ $ H \rightarrow L; H \rightarrow L; H-1 \rightarrow L+1\rangle (0.0929)$
II	$2^1B_{2u}^+$	2.65	0.897	0.047	$ H-1 \rightarrow L+1\rangle (-0.7244)$ $ H \rightarrow L+2\rangle + c.c.(0.2638)$
III	$3^1B_{2u}^+$	2.89	0.440	0.012	$ H \rightarrow L+2\rangle + c.c.(0.5326)$ $ H-1 \rightarrow L+1\rangle (-0.3290)$
	$1^1B_{3u}^+$	2.97	0.845	0.046	$ H \rightarrow L; H \rightarrow L+1\rangle - c.c.(0.4942)$ $ H \rightarrow L+1; H-1 \rightarrow L+1\rangle - c.c.(0.2522)$
IV	$2^1B_{3u}^+$	3.38	3.675	1.000	$ H \rightarrow L+4\rangle + c.c.(0.5831)$ $ H-1 \rightarrow L+5\rangle + c.c.(0.1004)$
V	$3^1B_{3u}^+$	3.91	0.410	0.014	$ H \rightarrow L+1; H \rightarrow L+2\rangle - c.c.(0.4028)$ $ H \rightarrow L+1; H \rightarrow L+4\rangle - c.c.(0.3003)$
	$4^1B_{2u}^+$	3.97	0.641	0.036	$ H-2 \rightarrow L+2\rangle (-0.5280)$ $ H-1 \rightarrow L+3\rangle + c.c.(0.3722)$
VI	$8^1B_{2u}^+$	4.52	0.230	0.005	$ H \rightarrow L; H \rightarrow L+5\rangle - c.c.(0.4706)$ $ H \rightarrow L; H-1 \rightarrow L+4\rangle - c.c.(0.3075)$
	$6^1B_{3u}^+$	4.57	0.403	0.016	$ H \rightarrow L; H \rightarrow L+1\rangle - c.c.(0.3419)$ $ H \rightarrow L; H \rightarrow L+3\rangle - c.c.(0.2890)$
VII	$8^1B_{3u}^+$	4.80	1.301	0.178	$ H-1 \rightarrow L+5\rangle + c.c.(0.5537)$ $ H \rightarrow L; H-1 \rightarrow L+2\rangle - c.c.(0.1321)$
VIII	$9^1B_{3u}^+$	5.14	0.410	0.019	$ H-2 \rightarrow L+4\rangle + c.c.(0.5720)$ $ H \rightarrow L+2; H \rightarrow L+3\rangle - c.c.(0.0943)$
	$13^1B_{2u}^+$	5.22	0.418	0.020	$ H \rightarrow L; H-1 \rightarrow L+1; H-1 \rightarrow L+1\rangle (0.3505)$ $ H-1 \rightarrow L+7\rangle + c.c.(0.2709)$
IX	$16^1B_{2u}^+$	5.53	0.440	0.023	$ H-1 \rightarrow L+7\rangle + c.c.(0.3983)$ $ H-3 \rightarrow L+3\rangle (0.3636)$
	$12^1B_{3u}^+$	5.66	0.154	0.003	$ H \rightarrow L; H-1 \rightarrow L+6\rangle - c.c.(0.4014)$ $ H \rightarrow L+2; H-2 \rightarrow L+1\rangle - c.c.(0.3019)$

Table 8: Excited states contributing to the singlet linear absorption spectrum of nonacene computed using the MRSDCI method coupled with the standard parameters in the PPP model Hamiltonian. The rest of the information is same as that in Table 6.

Peak	State	E (eV)	Transition Dipole (Å)	ROS	dominant contributing configurations
DF	$1^1B_{3u}^-$	1.86	0	0	$ H \rightarrow L; H \rightarrow L+1\rangle + c.c.(0.4872)$ $ H \rightarrow L+1; H \rightarrow L+2\rangle + c.c.(0.2027)$
I	$1^1B_{2u}^+$	1.82	1.328	0.092	$ H \rightarrow L\rangle (0.8290)$ $ H \rightarrow L; H \rightarrow L; H-1 \rightarrow L+1\rangle (0.1066)$
II	$2^1B_{2u}^+$	2.79	0.733	0.043	$ H-1 \rightarrow L+1\rangle (0.5506)$ $ H \rightarrow L+2\rangle + c.c.(0.4342)$
III	$1^1B_{3u}^+$	3.80	3.037	1.000	$ H \rightarrow L+4\rangle - c.c.(0.3757)$ $ H \rightarrow L; H \rightarrow L+1\rangle - c.c.(0.3274)$
IV	$2^1B_{3u}^+$	4.12	2.583	0.786	$ H \rightarrow L+4\rangle - c.c.(0.3943)$ $ H \rightarrow L; H \rightarrow L+1\rangle - c.c.(0.2791)$
V	$5^1B_{2u}^+$	4.62	0.439	0.025	$ H \rightarrow L; H \rightarrow L; H-1 \rightarrow L+1\rangle (0.6215)$ $ H-1 \rightarrow L+1\rangle (0.2357)$
	$3^1B_{3u}^+$	4.63	0.549	0.040	$ H \rightarrow L+1; H-1 \rightarrow L+1\rangle - c.c.(0.3339)$ $ H \rightarrow L+1; H \rightarrow L+2\rangle - c.c.(0.3035)$
VI	$10^1B_{2u}^+$	5.29	0.457	0.032	$ H-2 \rightarrow L+2\rangle (-0.3824)$ $ H \rightarrow L+1; H \rightarrow L+4\rangle + c.c.(0.2681)$
VII	$7^1B_{3u}^+$	5.71	0.277	0.013	$ H \rightarrow L+8\rangle - c.c.(0.3021)$ $ H \rightarrow L; H \rightarrow L+3\rangle + c.c.(0.2619)$
	$12^1B_{2u}^+$	5.72	0.318	0.017	$ H \rightarrow L; H-1 \rightarrow L+1; H-1 \rightarrow L+1\rangle (-0.3293)$ $ H \rightarrow L; H-1 \rightarrow L+4\rangle - c.c.(0.2869)$
VIII	$16^1B_{2u}^+$	5.94	0.287	0.014	$ H \rightarrow L; H \rightarrow L+2; H-1 \rightarrow L+1\rangle - c.c.(0.3742)$ $ H \rightarrow L; H-1 \rightarrow L+4\rangle - c.c.(0.2500)$
	$8^1B_{3u}^+$	5.95	0.996	0.169	$ H-1 \rightarrow L+5\rangle - c.c.(0.3932)$ $ H-2 \rightarrow L+4\rangle - c.c.(0.2993)$

Table 9: Excited states contributing to the singlet linear absorption spectrum of nonacene computed using the MRSDCI method coupled with the screened parameters in the PPP model Hamiltonian. The rest of the information is same as that in Table 6.

Peak	State	E (eV)	Transition	ROS	dominant contributing configurations
Dipole (Å)					
DF	$1^1B_{3u}^-$	1.51	0	0	$ H \rightarrow L; H \rightarrow L+1\rangle + c.c.(0.5143)$ $ H \rightarrow L; H-1 \rightarrow L+2\rangle - c.c.(0.2089)$
I	$1^1B_{2u}^+$	1.46	1.316	0.051	$ H \rightarrow L\rangle (0.8551)$ $ H \rightarrow L; H \rightarrow L; H-1 \rightarrow L+1\rangle (0.1017)$
II	$2^1B_{2u}^+$	2.45	0.935	0.043	$ H-1 \rightarrow L+1\rangle (0.7260)$ $ H \rightarrow L+2\rangle - c.c.(0.2689)$
III	$1^1B_{3u}^+$	2.71	0.611	0.020	$ H \rightarrow L; H \rightarrow L+1\rangle - c.c.(0.4901)$ $ H \rightarrow L+1; H-1 \rightarrow L+1\rangle - c.c.(0.2454)$
	$3^1B_{2u}^+$	2.77	0.507	0.014	$ H \rightarrow L+2\rangle - c.c.(0.5434)$ $ H-1 \rightarrow L+1\rangle (-0.3462)$
IV	$2^1B_{3u}^+$	3.32	3.887	1.000	$ H \rightarrow L+4\rangle - c.c.(0.5689)$ $ H-1 \rightarrow L+6\rangle + c.c.(0.1185)$
V	$3^1B_{3u}^+$	3.63	0.782	0.044	$ H \rightarrow L+1; H \rightarrow L+2\rangle + c.c.(0.3441)$ $ H-1 \rightarrow L+1; H \rightarrow L+1\rangle - c.c.(0.3221)$
	$4^1B_{2u}^+$	3.69	0.559	0.023	$ H-2 \rightarrow L+2\rangle (-0.4715)$ $ H-1 \rightarrow L+3\rangle + c.c.(0.4395)$
VI	$4^1B_{3u}^+$	3.93	0.369	0.011	$ H \rightarrow L; H-1 \rightarrow L+2\rangle - c.c.(0.4953)$ $ H \rightarrow L; H \rightarrow L+3\rangle - c.c.(0.2163)$
	$6^1B_{2u}^+$	4.01	0.690	0.038	$ H \rightarrow L; H \rightarrow L; H-1 \rightarrow L+1\rangle (0.5954)$ $ H \rightarrow L+5\rangle + c.c.(0.3166)$
	$7^1B_{2u}^+$	4.12	0.692	0.039	$ H-2 \rightarrow L+2\rangle (-0.5949)$ $ H-1 \rightarrow L+3\rangle + c.c.(0.3994)$
VII	$8^1B_{3u}^+$	4.61	1.450	0.193	$ H-1 \rightarrow L+6\rangle + c.c.(0.5262)$ $ H \rightarrow L; H-1 \rightarrow L+2\rangle - c.c.(0.1473)$
VIII	$9^1B_{3u}^+$	4.97	0.338	0.011	$ H-2 \rightarrow L+4\rangle + c.c.(0.5823)$ $ H \rightarrow L+8\rangle + c.c.(0.0699)$

Table 10: Excited states contributing to the singlet linear absorption spectrum of decacene computed using the MRSDCI method coupled with the standard parameters in the PPP model Hamiltonian. The rest of the information is same as that in Table 6.

Peak	State	E (eV)	Transition Dipole (Å)	ROS	dominant contributing configurations
DF	$1^1B_{3u}^-$	1.72	0	0	$ H \rightarrow L; H \rightarrow L+1\rangle - c.c.(0.4790)$ $ H \rightarrow L+1; H \rightarrow L+2\rangle + c.c.(0.2119)$
I	$1^1B_{2u}^+$	1.79	1.423	0.084	$ H \rightarrow L\rangle (-0.8203)$ $ H-1 \rightarrow L+1\rangle (-0.1213)$
II	$2^1B_{2u}^+$	2.64	0.776	0.037	$ H-1 \rightarrow L+1\rangle (-0.5607)$ $ H \rightarrow L+2\rangle - c.c.(0.4239)$
III	$1^1B_{3u}^+$	3.68	2.554	0.553	$ H \rightarrow L; H \rightarrow L+1\rangle + c.c.(0.3710)$ $ H \rightarrow L+4\rangle + c.c.(0.2865)$
IV	$2^1B_{3u}^+$	4.00	3.293	1.000	$ H \rightarrow L+4\rangle + c.c.(0.4451)$ $ H \rightarrow L+1; H \rightarrow L+2\rangle - c.c.(0.2322)$
V	$5^1B_{2u}^+$	4.40	0.505	0.026	$ H \rightarrow L; H \rightarrow L; H-1 \rightarrow L+1\rangle (-0.6203)$ $ H-1 \rightarrow L+1\rangle (-0.2380)$
	$3^1B_{3u}^+$	4.46	0.739	0.056	$ H \rightarrow L+1; H-1 \rightarrow L+1\rangle + c.c.(0.3459)$ $ H \rightarrow L+1; H \rightarrow L+2\rangle - c.c.(0.2800)$
VI	$9^1B_{2u}^+$	5.05	0.392	0.018	$ H-2 \rightarrow L+2\rangle (-0.3901)$ $ H-1 \rightarrow L+3\rangle (-0.2482)$
VII	$6^1B_{3u}^+$	5.45	0.337	0.014	$ H \rightarrow L; H-1 \rightarrow L+2\rangle - c.c.(0.3992)$ $ H \rightarrow L+8\rangle - c.c.(0.2341)$
	$11^1B_{2u}^+$	5.45	0.351	0.015	$ H \rightarrow L; H-1 \rightarrow L+1; H-1 \rightarrow L+1\rangle (-0.4912)$ $ H \rightarrow L; H \rightarrow L; H-1 \rightarrow L+1\rangle (-0.2510)$
VIII	$7^1B_{3u}^+$	5.59	0.584	0.044	$ H \rightarrow L+8\rangle (0.3796)$ $ H-1 \rightarrow L+6\rangle - c.c.(0.2866)$
	$14^1B_{2u}^+$	5.62	0.332	0.014	$ H \rightarrow L+12\rangle + c.c.(0.4160)$ $ H-1 \rightarrow L+7\rangle + c.c.(0.2309)$
	$15^1B_{2u}^+$	5.63	0.326	0.014	$ H \rightarrow L+9\rangle + c.c.(0.3036)$ $ H-1 \rightarrow L+7\rangle + c.c.(0.2945)$
IX	$8^1B_{3u}^+$	5.89	0.913	0.113	$ H-2 \rightarrow L+4\rangle - c.c.(0.3596)$ $ H-1 \rightarrow L+6\rangle - c.c.(0.2949)$
	$17^1B_{2u}^+$	5.89	0.149	0.003	$ H \rightarrow L; H-1 \rightarrow L+4\rangle - c.c.(0.4687)$ $ H \rightarrow L; H \rightarrow L; H-2 \rightarrow L+2\rangle (-0.1847)$

Table 11: Excited states contributing to the singlet linear absorption spectrum of decacene computed using the MRSDCI method coupled with the screened parameters in the PPP model Hamiltonian. The rest of the information is same as that in Table 6.

Peak	State	E (eV)	Transition	ROS	dominant contributing configurations
Dipole (\AA)					
DF	$1^1B_{3u}^-$	1.15	0	0	$ H \rightarrow L; H \rightarrow L+1\rangle - c.c.(0.4851)$ $ H \rightarrow L+1; H-1 \rightarrow L+2\rangle - c.c.(0.2102)$
I	$1^1B_{2u}^+$	1.27	1.369	0.067	$ H \rightarrow L\rangle (-0.8338)$ $ H \rightarrow L; H \rightarrow L; H-1 \rightarrow L+1\rangle (+0.1112)$
II	$2^1B_{2u}^+$	2.16	0.929	0.052	$ H-1 \rightarrow L+1\rangle (+0.7110)$ $ H \rightarrow L+2\rangle + c.c.(0.2625)$
III	$3^1B_{2u}^+$	2.42	0.417	0.012	$ H \rightarrow L+2\rangle + c.c.(0.5220)$ $ H-1 \rightarrow L+1\rangle (-0.3185)$
	$1^1B_{3u}^+$	2.42	0.295	0.006	$ H \rightarrow L; H \rightarrow L+1\rangle + c.c.(0.4762)$ $ H-1 \rightarrow L; H-1 \rightarrow L+1\rangle + c.c.(0.2590)$
IV	$2^1B_{3u}^+$	3.20	1.872	0.315	$ H \rightarrow L+1; H \rightarrow L+2\rangle + c.c.(0.3455)$ $ H \rightarrow L+5\rangle + c.c.(0.2733)$
	$4^1B_{2u}^+$	3.21	0.706	0.045	$ H-2 \rightarrow L+2\rangle (0.5140)$ $ H-1 \rightarrow L+3\rangle + c.c.(0.3975)$
V	$4^1B_{3u}^+$	3.35	3.259	1.000	$ H \rightarrow L+5\rangle + c.c.(0.4970)$ $ H \rightarrow L; H-1 \rightarrow L+2\rangle - c.c.(0.2002)$
VI	$6^1B_{3u}^+$	3.81	0.273	0.008	$ H \rightarrow L; H \rightarrow L+1\rangle - c.c.(0.3703)$ $ H \rightarrow L; H \rightarrow L+3\rangle + c.c.(0.3689)$
VII	$8^1B_{3u}^+$	4.32	0.184	0.004	$ H \rightarrow L; H-1 \rightarrow L+4\rangle - c.c.(0.2891)$ $ H \rightarrow L+6; H-5 \rightarrow L+2\rangle - c.c.(0.2750)$
	$10^1B_{2u}^+$	4.33	0.478	0.028	$ H-1 \rightarrow L+7\rangle - c.c.(0.2951)$ $ H-2 \rightarrow L+4\rangle - c.c.(0.2793)$
VIII	$9^1B_{3u}^+$	4.51	0.330	0.014	$ H \rightarrow L+8\rangle + c.c.(0.4467)$ $ H \rightarrow L+2; H-1 \rightarrow L+2\rangle + c.c.(0.2155)$
	$14^1B_{2u}^+$	4.56	0.376	0.018	$ H \rightarrow L+9\rangle + c.c.(0.4944)$ $ H-3 \rightarrow L+7\rangle (-0.2478)$
IX	$11^1B_{3u}^+$	4.77	0.754	0.076	$ H-2 \rightarrow L+5\rangle + c.c.(0.5543)$ $ H \rightarrow L+3; H-1 \rightarrow L+1\rangle - c.c.(0.2076)$
	$16^1B_{2u}^+$	4.77	0.520	0.036	$ H-1 \rightarrow L+7\rangle - c.c.(0.3795)$ $ H-3 \rightarrow L+7\rangle (0.3359)$

Triplet absorption

In the following we present a detailed description of the calculated triplet absorption spectra of octacene, nonacene, and decacene, presented in Figures 8-10 of the main text for the standard and the screened parameters.

1. The first peak always corresponds to the $1^3B_{1g}^-$ excited state of the system, whose wave function is dominated by the single excitations $|H \rightarrow L+1\rangle + c.c.$, irrespective of the oligoacene in question, or the Coulomb parameters employed.
2. The second peak corresponds to a y-polarized transition to the $1^3A_g^-$ excited state, for all the oligoacenes, irrespective of the Coulomb parameters employed. The most important configuration contributing to the many-particle wave function of the $1^3A_g^-$ state, is the double excitation $|H \rightarrow L; H-1 \rightarrow L+1\rangle$.
3. The nature of the third peak is dependent upon the Coulomb parameters employed in the PPP model. For the standard parameter case, this peak corresponds to a mixture of x- and y-polarized the transitions to states, $2^3B_{1g}^-$ and $3^3A_g^-$ for octacene and nonacene. For octacene, the single excitations $|H \rightarrow L+4\rangle + c.c.$ for the $2^3B_{1g}^-$ state, and $|H-1 \rightarrow L+3\rangle + c.c.$ for $3^3A_g^-$ state contribute the most to the respective wave functions. For nonacene, the single excitations $|H \rightarrow L+3\rangle + c.c.$ for the $2^3B_{1g}^-$ state, and the double excitation $|H \rightarrow L; H-1 \rightarrow L+1\rangle$ for the $3^3A_g^-$ states dominate the corresponding wave functions. However, for decacene, the peak corresponds to an x polarized transition to the state $2^3B_{1g}^-$, whose wave function is dominated by single excitations, with the configurations $|H \rightarrow L+3\rangle + c.c.$ contributing the most.

For the screened parameter case, for all the oligomers, the third peak is due to an x -polarized transition to the state $3^3B_{1g}^-$ whose wave function derives the maximum contribution from the single excitations $|H \rightarrow L+3\rangle + c.c..$

4. As far as the fourth peak is concerned, with standard parameters it corresponds to an x -polarized transition to the $3^3B_{1g}^-$ excited state, for all the oligoacenes. For octacene, it happens to be the most intense peak of the spectrum, but for nonacene and decacene, it is a shoulder to the most intense peak. Double excitations $|H \rightarrow L; H \rightarrow L+3\rangle + c.c.$ contribute the most to the many-particle wave function of this state for octacene, whereas for nonacene and decacene, the single excitations $|H-1 \rightarrow L+2\rangle + c.c.$ dominate the wave function.

In the screened parameter spectrum, the fourth peak is due to a y -polarized transition to the $3^3A_g^-$ state for octacene and nonacene. For octacene, the single excitations $|H \rightarrow L+5\rangle + c.c.$ contribute the most to the many particle wave function of this state, while for nonacene, the single excitations $|H \rightarrow L+6\rangle + c.c.$ dominate the state. However, for decacene, the fourth peak is the second most intense peak of the spectrum, corresponding to an x -polarized transition to the $6^3B_{1g}^-$ state, whose wave function is dominated by the double excitations $|H \rightarrow L; H \rightarrow L+5\rangle + c.c..$

5. For the standard parameter case, the fifth peak is due to an x -polarized transition to the state $4^3B_{1g}^-$ for all the oligoacenes. For the case of octacene, it appears as a shoulder of the most intense peak (peak IV), while for nonacene and decacene it is the most intense peak. For octacene the wave function of this state is composed mainly of single excitations, with configurations $|H-1 \rightarrow L+2\rangle + c.c.$ contributing the most. For nonacene and decacene, however, the wave function is dominated by the double excitations $|H \rightarrow L; H \rightarrow L+4\rangle + c.c..$

In the screened parameter spectrum also the fifth peak corresponds to an x polarized transition for all the oligomers. For octacene, nonacene, and decacene, the states involved

are $4^3B_{1g}^-$, $6^3B_{1g}^-$, and $8^3B_{1g}^-$, respectively. For octacene and nonacene, this peak is the second most intense one of the corresponding spectra, and the most important configuration contributing to the many-particle wave function of the states are the double excitations $|H \rightarrow L; H \rightarrow L+4\rangle + c.c.$. However, for decacene, it is a relatively weaker feature, with the double excitations $|H-1 \rightarrow L; H \rightarrow L+6\rangle + c.c.$ dominating the wave function of the state.

6. The sixth peak in the standard parameter spectrum, is formed by a y -polarized transition to the state $9^3A_g^-$ for the case of octacene, whose wave function is dominated by the single excitations $|H \rightarrow L+5\rangle + c.c.$ and $|H-3 \rightarrow L+1\rangle + c.c.$ However, for nonacene and decacene, it corresponds to an x -polarized transition to the state $6^3B_{1g}^-$, whose wave function receives maximum contribution from the triple excitations $|H \rightarrow L+1; H \rightarrow L+1; H-1 \rightarrow L\rangle + c.c.$.

With the screened parameters, this peak is formed by an x -polarized transition to the state $7^3B_{1g}^-$ for octacene, with double excitations $|H \rightarrow L+1; H-5 \rightarrow L\rangle + c.c.$ dominating its wave function. For nonacene and decacene, the peak is due to mixed x and y polarized transitions. For nonacene, states $8^3B_{1g}^-$ and $10^3A_g^-$ form this peak, with their wave functions dominated by double excitations $|H \rightarrow L+1; H-6 \rightarrow L+1\rangle + c.c.$, and $|H-1 \rightarrow L+1; H \rightarrow L+2\rangle + c.c.$, respectively. For decacene, the states involved are $11^3B_{1g}^-$ and $14^3A_g^-$, with their wave functions dominated by the double excitations $|H \rightarrow L+1; H-1 \rightarrow L+5\rangle + c.c.$, and single excitations $|H-1 \rightarrow L+8\rangle + c.c.$, respectively.

7. With the the standard parameters, peak VII for octacene corresponds to an x -polarized transition to the state $7^3B_{1g}^-$ with the double excitations $|H \rightarrow L; H-2 \rightarrow L+3\rangle + c.c.$ dominating its wave function. However, for nonacene and decacene this peak corresponds to a mixed x - and y -polarized transition. For nonacene, the states involved are $7^3B_{1g}^-$ and $11^3A_g^-$, with the double excitations $|H \rightarrow L+1; H-5 \rightarrow L\rangle + c.c.$, and single excitations $|H \rightarrow L+5\rangle + c.c.$, contributing the most to their respective wave functions. For decacene, the states forming the peak are $8^3B_{1g}^-$ and $11^3A_g^-$, of which the former is dominated by the double and triple

excitations, while the latter consists mainly of the single excitations.

Screened parameter calculations predict peak VII to have a mixed x and y polarized character for all the oligomers. For the case of octacene, four states $11^3B_{1g}^-$, $12^3B_{1g}^-$, $11^3A_g^-$, and $12^3A_g^-$, form this peak and the double excitations dominate the wave function of the first three states, while $12^3A_g^-$ is dominated by the single excitations. For nonacene, two states $11^3B_{1g}^-$ and $12^3A_g^-$ shape the peak with the triple excitations ($|H \rightarrow L; H \rightarrow L; H - 1 \rightarrow L + 2\rangle + c.c.$) dominating the wave function of the former, and single excitations ($|H - 1 \rightarrow L + 8\rangle + c.c.$) that of the latter. For decacene, three states, $13^3B_{1g}^-$, $14^3B_{1g}^-$, and $15^3A_g^-$, contribute to the peak, with the double excitations dominating all their wave functions.

8. In the standard parameter spectrum, peak VIII has a mixed x and y polarized character for octacene, but only a y -polarized character for nonacene and decacene. For octacene, the peak is formed by states $8^3B_{1g}^-$ and $12^3A_g^-$, of which the wave function of the former is dominated by the triple and double excitations, while that of the latter by double and single excitations. For nonacene, the state in question is $13^3A_g^-$, while for decacene it is $12^3A_g^-$, and wave functions in both the cases are dominated by doubly-excited configurations.

In the screened parameter calculations, peak VIII exists only for octacene and nonacene, and is due to an x -polarized transition. For octacene it is formed by the state $13^3B_{1g}^-$, whose wave function is dominated by both single and double excitations. For nonacene, the peak is caused by the state $12^3B_{1g}^-$, whose wave function mainly consists of double excitations.

Table 12: Excited states contributing to the triplet absorption spectrum of octacene computed using the MRSDCI method coupled with the standard parameters in the PPP model Hamiltonian. The table includes many-particle dominant contributing configurations, excitation energies, dipole matrix elements, and relative oscillator strengths (ROS) of various states. The excitation energies are with respect to the $1^1A_g^-$, ground state, while the dipole matrix elements, and the ROS, are with respect to the $1^3B_{2u}^+$ state. Below, ‘+c.c.’ indicates that the coefficient of charge conjugate of a given configuration has the same sign, while ‘-c.c.’ implies that the two coefficients have opposite signs.

Peak	State	E (eV)	Transition Dipole (Å)	ROS	dominant contributing configurations
I	$1^3B_{1g}^-$	3.04	2.950	0.839	$ H \rightarrow L+1\rangle - c.c.(0.5638)$ $ H-1 \rightarrow L+2\rangle + c.c.(0.1836)$
II	$1^3A_g^-$	3.89	0.997	0.123	$ H \rightarrow L; H-1 \rightarrow L+1\rangle (0.8187)$ $ H \rightarrow L; H-2 \rightarrow L+2\rangle (0.1135)$
III	$3^3A_g^-$	4.28	0.355	0.017	$ H-1 \rightarrow L+3\rangle - c.c.(0.3698)$ $ H \rightarrow L+5\rangle - c.c.(0.3435)$
	$2^3B_{1g}^-$	4.35	0.579	0.046	$ H \rightarrow L+4\rangle - c.c.(0.5362)$ $ H-1 \rightarrow L+2\rangle + c.c.(0.1999)$
IV	$3^3B_{1g}^-$	5.06	2.494	1.000	$ H \rightarrow L; H \rightarrow L+3\rangle - c.c.(0.4566)$ $ H-1 \rightarrow L+2\rangle + c.c.(0.3011)$
V	$4^3B_{1g}^-$	5.26	1.199	0.240	$ H-1 \rightarrow L+2\rangle + c.c.(0.3688)$ $ H \rightarrow L; H \rightarrow L+3\rangle - c.c.(0.2757)$
VI	$9^3A_g^-$	5.82	0.588	0.064	$ H \rightarrow L+5\rangle - c.c.(0.3967)$ $ H-3 \rightarrow L+1\rangle - c.c.(0.3809)$
VII	$7^3B_{1g}^-$	6.10	1.055	0.216	$ H \rightarrow L; H-2 \rightarrow L+3\rangle - c.c.(0.4326)$ $ H \rightarrow L+1; H-1 \rightarrow L+3\rangle - c.c.(0.1274)$
VIII	$8^3B_{1g}^-$	6.29	0.864	0.149	$ H \rightarrow L+1; H \rightarrow L+1; H-1 \rightarrow L\rangle - c.c.(0.4030)$ $ H \rightarrow L; H-2 \rightarrow L+3\rangle - c.c.(0.3504)$
	$12^3A_g^-$	6.29	0.149	0.004	$ H-1 \rightarrow L+1; H \rightarrow L+2\rangle - c.c.(0.3707)$ $ H-3 \rightarrow L+4\rangle - c.c.(0.2968)$

Table 13: Excited states contributing to the triplet absorption spectrum of octacene computed using the MRSDCI method coupled with the screened parameters in the PPP model Hamiltonian. The rest of the information is same as that in Table 12.

Peak	State	E (eV)	Transition Dipole (Å)	ROS	dominant contributing configurations
I	$1^3B_{1g}^-$	1.97	4.639	1.000	$ H \rightarrow L+1\rangle + c.c.(0.5936)$
II	$1^3A_g^-$	2.92	0.996	0.064	$ H-1 \rightarrow L+2\rangle + c.c.(0.0990)$ $ H \rightarrow L; H-1 \rightarrow L+1\rangle (0.8333)$
III	$3^3B_{1g}^-$	3.39	0.465	0.017	$ H-1 \rightarrow L; H-1 \rightarrow L+2\rangle - c.c.(0.1090)$ $ H \rightarrow L+3\rangle + c.c.(0.4280)$
IV	$3^3A_g^-$	3.68	0.621	0.034	$ H-1 \rightarrow L+2\rangle + c.c.(0.3614)$ $ H \rightarrow L+5\rangle + c.c.(0.4915)$
V	$4^3B_{1g}^-$	4.01	2.601	0.641	$ H-1 \rightarrow L+4\rangle + c.c.(0.3220)$ $ H \rightarrow L; H \rightarrow L+4\rangle - c.c.(0.5605)$
VI	$7^3B_{1g}^-$	4.67	1.017	0.114	$ H \rightarrow L+1; H-1 \rightarrow L+4\rangle - c.c.(0.1764)$ $ H \rightarrow L+1; H-5 \rightarrow L\rangle - c.c.(0.5190)$
VII	$11^3A_g^-$	5.13	0.151	0.003	$ H-1 \rightarrow L+1; H \rightarrow L+2\rangle - c.c.(0.3311)$ $ H-1 \rightarrow L+8\rangle - c.c.(0.2700)$
	$11^3B_{1g}^-$	5.15	0.768	0.072	$ H \rightarrow L+1; H-1 \rightarrow L+4\rangle - c.c.(0.4913)$ $ H \rightarrow L+1; H-5 \rightarrow L\rangle - c.c.(0.2874)$
	$12^3B_{1g}^-$	5.18	0.345	0.015	$ H \rightarrow L+1; H-5 \rightarrow L\rangle - c.c.(0.4987)$ $ H \rightarrow L+1; H-1 \rightarrow L+4\rangle - c.c.(0.2693)$
	$12^3A_g^-$	5.19	0.148	0.003	$ H-1 \rightarrow L+8\rangle + c.c.(0.3959)$ $ H \rightarrow L; H-1 \rightarrow L+3\rangle - c.c.(0.2687)$
VIII	$13^3B_{1g}^-$	5.39	0.777	0.077	$ H-1 \rightarrow L+8\rangle + c.c.(0.3959)$ $ H \rightarrow L; H-1 \rightarrow L+3\rangle - c.c.(0.2687)$

Table 14: Excited states contributing to the triplet absorption spectrum of nonacene computed using the MRSDCI method coupled with the standard parameters in the PPP model Hamiltonian. The rest of the information is same as that in Table 12.

Peak	State	E (eV)	Transition Dipole (Å)	ROS	dominant contributing configurations
I	$1^3B_{1g}^-$	2.56	3.331	0.785	$ H \rightarrow L+1\rangle + c.c.(0.5522)$ $ H-1 \rightarrow L+2\rangle + c.c.(0.1825)$
II	$1^3A_g^-$	3.30	1.018	0.095	$ H \rightarrow L; H-1 \rightarrow L+1\rangle (0.8148)$ $ H \rightarrow L; H-1 \rightarrow L+3\rangle c.c.(0.1109)$
III	$2^3B_{1g}^-$	3.79	0.686	0.049	$ H \rightarrow L+3\rangle - c.c.(0.5156)$ $ H-1 \rightarrow L+2\rangle + c.c.(0.2173)$
	$3^3A_g^-$	3.89	0.352	0.013	$ H \rightarrow L; H-1 \rightarrow L+1\rangle (0.4041)$ $ H-1 \rightarrow L+4\rangle - c.c.(0.3279)$
IV	$3^3B_{1g}^-$	4.39	0.790	0.076	$ H-1 \rightarrow L+2\rangle + c.c.(0.4226)$ $ H \rightarrow L; H \rightarrow L; H-1 \rightarrow L+2\rangle + c.c.(0.2222)$
V	$4^3B_{1g}^-$	4.66	2.789	1.000	$ H \rightarrow L; H \rightarrow L+4\rangle + c.c.(0.5047)$ $ H-1 \rightarrow L; H \rightarrow L+5\rangle - c.c.(0.2034)$
VI	$6^3B_{1g}^-$	5.14	0.418	0.025	$ H \rightarrow L+1; H \rightarrow L+1; H-1 \rightarrow L\rangle + c.c.(0.4111)$ $ H \rightarrow L; H \rightarrow L+4\rangle + c.c.(0.2905)$
VII	$11^3A_g^-$	5.39	0.517	0.040	$ H \rightarrow L+5\rangle - c.c.(0.3654)$ $ H-1 \rightarrow L+4\rangle - c.c.(0.3219)$
	$7^3B_{1g}^-$	5.44	1.438	0.310	$ H \rightarrow L+1; H-5 \rightarrow L\rangle - c.c.(0.4435)$ $ H \rightarrow L+1; H \rightarrow L+4\rangle - c.c.(0.3271)$
VIII	$13^3A_g^-$	5.75	0.428	0.029	$ H-1 \rightarrow L+1; H \rightarrow L+2\rangle - c.c.(0.2992)$ $ H \rightarrow L; H-1 \rightarrow L+3\rangle - c.c.(0.2305)$

Table 15: Excited states contributing to the triplet absorption spectrum of nonacene computed using the MRSDCI method coupled with the screened parameters in the PPP model Hamiltonian. The rest of the information is same as that in Table 12.

Peak	State	E (eV)	Transition Dipole (Å)	ROS	dominant contributing configurations
I	$1^3B_{1g}^-$	1.86	5.218	1.000	$ H \rightarrow L+1\rangle + c.c.(0.5919)$ $ H-1 \rightarrow L+2\rangle - c.c.(0.1143)$
II	$1^3A_g^-$	2.61	1.032	0.055	$ H \rightarrow L; H-1 \rightarrow L+1\rangle (0.8266)$ $ H-1 \rightarrow L; H \rightarrow L+2\rangle + c.c.(0.1122)$
III	$3^3B_{1g}^-$	3.14	0.711	0.031	$ H \rightarrow L+3\rangle + c.c.(0.4278)$ $ H-1 \rightarrow L+2\rangle - c.c.(0.3551)$
IV	$3^3A_g^-$	3.58	0.514	0.019	$ H \rightarrow L+6\rangle + c.c.(0.4657)$ $ H-1 \rightarrow L+4\rangle - c.c.(0.3453)$
V	$6^3B_{1g}^-$	4.09	2.577	0.535	$ H \rightarrow L; H \rightarrow L+4\rangle + c.c.(0.5088)$ $ H-1 \rightarrow L; H \rightarrow L+1; H \rightarrow L+1\rangle + c.c.(0.2302)$
VI	$10^3A_g^-$	4.52	0.324	0.009	$ H-1 \rightarrow L+1; H \rightarrow L+2\rangle - c.c.(0.3581)$ $ H \rightarrow L; H-1 \rightarrow L+3\rangle - c.c.(0.2788)$
	$8^3B_{1g}^-$	4.53	1.434	0.184	$ H \rightarrow L+1; H-6 \rightarrow L+1\rangle - c.c.(0.5621)$ $ H-2 \rightarrow L+3\rangle - c.c.(0.1869)$
VII	$11^3B_{1g}^-$	4.87	0.398	0.015	$ H \rightarrow L; H \rightarrow L; H-1 \rightarrow L+2\rangle - c.c.(0.4361)$ $ H-1 \rightarrow L; H-1 \rightarrow L; H \rightarrow L+1\rangle + c.c.(0.3273)$
	$12^3A_g^-$	4.92	0.215	0.004	$ H-1 \rightarrow L+8\rangle + c.c.(0.4643)$ $ H \rightarrow L; H-1 \rightarrow L+3\rangle - c.c.(0.2204)$
VIII	$12^3B_{1g}^-$	5.14	0.884	0.079	$ H \rightarrow L+1; H-6 \rightarrow L+1\rangle - c.c.(0.5873)$ $ H \rightarrow L; H-1 \rightarrow L+2\rangle - c.c.(0.0756)$

Table 16: Excited states contributing to the triplet absorption spectrum of decacene computed using the MRSDCI method coupled with the standard parameters in the PPP model Hamiltonian. The rest of the information is same as that in Table 12.

Peak	State	E (eV)	Transition Dipole (Å)	ROS	dominant contributing configurations
I	$1^3B_{1g}^-$	2.49	3.615	1.000	$ H \rightarrow L+1\rangle - c.c.(0.5461)$ $ H-1 \rightarrow L+2\rangle + c.c.(0.1918)$
II	$1^3A_g^-$	3.16	1.097	0.117	$ H \rightarrow L; H-1 \rightarrow L+1\rangle (0.8189)$ $ H \rightarrow L; H-1 \rightarrow L+3\rangle - c.c.(0.1177)$
III	$2^3B_{1g}^-$	3.62	0.800	0.071	$ H \rightarrow L+3\rangle - c.c.(0.5228)$ $ H-1 \rightarrow L+2\rangle + c.c.(0.1965)$
IV	$3^3B_{1g}^-$	4.35	0.793	0.084	$ H-1 \rightarrow L+2\rangle + c.c.(0.4745)$ $ H-1 \rightarrow L+4\rangle - c.c.(0.1760)$
V	$4^3B_{1g}^-$	4.62	2.534	0.912	$ H \rightarrow L; H \rightarrow L+4\rangle - c.c.(0.4009)$ $ H \rightarrow L+7\rangle - c.c.(0.2788)$
VI	$6^3B_{1g}^-$	5.22	1.183	0.225	$ H \rightarrow L+1; H \rightarrow L+1; H-1 \rightarrow L\rangle - c.c.(0.3604)$ $ H \rightarrow L+1; H-6 \rightarrow L\rangle - c.c.(0.3314)$
VII	$11^3A_g^-$	5.42	0.493	0.040	$ H \rightarrow L+6\rangle + c.c.(0.3537)$ $ H-1 \rightarrow L+4\rangle - c.c.(0.3086)$
	$8^3B_{1g}^-$	5.44	1.179	0.232	$ H \rightarrow L+1; H-1 \rightarrow L; H-1 \rightarrow L\rangle - c.c.(0.3928)$ $ H \rightarrow L+1; H-6 \rightarrow L\rangle - c.c.(0.3365)$
VIII	$12^3A_g^-$	5.70	0.456	0.036	$ H-1 \rightarrow L+1; H \rightarrow L+2\rangle - c.c.(0.3473)$ $ H \rightarrow L+1; H \rightarrow L+3\rangle - c.c.(0.2317)$

Table 17: Excited states contributing to the triplet absorption spectrum of decacene computed using the MRSDCI method coupled with the screened parameters in the PPP model Hamiltonian. The rest of the information is same as that in Table 12.

Peak	State	E (eV)	Transition Dipole (Å)	ROS	dominant contributing configurations
I	$1^3B_{1g}^-$	1.72	5.841	1.000	$ H \rightarrow L+1\rangle - c.c.(0.5872)$ $ H-1 \rightarrow L+2\rangle - c.c.(0.1112)$
II	$1^3A_g^-$	2.33	1.074	0.046	$ H \rightarrow L; H-1 \rightarrow L+1\rangle (0.8198)$ $ H \rightarrow L; H-1 \rightarrow L+2\rangle - c.c.(0.0986)$
III	$3^3B_{1g}^-$	2.89	0.831	0.034	$ H \rightarrow L+3\rangle - c.c.(0.4352)$ $ H-1 \rightarrow L+2\rangle - c.c.(0.3443)$
IV	$6^3B_{1g}^-$	3.80	2.695	0.470	$ H \rightarrow L; H \rightarrow L+5\rangle - c.c.(0.5362)$ $ H \rightarrow L+1; H-1 \rightarrow L+5\rangle - c.c.(0.1922)$
V	$8^3B_{1g}^-$	4.24	1.266	0.116	$ H-1 \rightarrow L; H \rightarrow L+6\rangle - c.c.(0.4998)$ $ H \rightarrow L+1; H-1 \rightarrow L+5\rangle - c.c.(0.3005)$
VI	$11^3B_{1g}^-$	4.70	0.791	0.050	$ H \rightarrow L+1; H-1 \rightarrow L+5\rangle - c.c.(0.4721)$ $ H \rightarrow L+1; H-6 \rightarrow L\rangle - c.c.(0.3044)$
	$14^3A_g^-$	4.72	0.135	0.001	$ H-1 \rightarrow L+8\rangle - c.c.(0.4705)$ $ H-3 \rightarrow L+5\rangle - c.c.(0.2190)$
VII	$13^3B_{1g}^-$	4.90	1.001	0.084	$ H \rightarrow L+1; H-5 \rightarrow L+1\rangle - c.c.(0.3314)$ $ H \rightarrow L+13\rangle - c.c.(0.3095)$
	$14^3B_{1g}^-$	4.91	0.638	0.034	$ H \rightarrow L+13\rangle - c.c.(0.4517)$ $ H \rightarrow L+1; H-5 \rightarrow L+1\rangle - c.c.(0.2219)$
	$15^3A_g^-$	4.91	0.162	0.002	$ H-1 \rightarrow L+1; H \rightarrow L+4\rangle - c.c.(0.4666)$ $ H-1 \rightarrow L+1; H-2 \rightarrow L+2\rangle (0.4449)$

This material is available free of charge via the Internet at <http://pubs.acs.org/>.

References

- (1) Clar, E. *Polycyclic Hydrocarbons*; Academic Press, 1964.
- (2) Clar, E. *The Aromatic Sextet*; J. Wiley, 1972.
- (3) Cooke, M.; Dennis, A.; Institute, E. P. R.; Agency, U. S. E. P.; Institute, A. P. *Polynuclear Aromatic Hydrocarbons: A Decade of Progress*; Battelle Press, 1988.
- (4) Harvey, R. *Polycyclic Aromatic Hydrocarbons: Chemistry and Carcinogenicity*; Cambridge University Press, 1991.
- (5) Bjørseth, A. *Handbook of Polycyclic Aromatic Hydrocarbons*; Dekker, 1983.
- (6) Müllen, K.; Wegner, G. *Electronic Materials: The Oligomer Approach*; Wiley-VCH, 1998.
- (7) Bendikov, M.; Wudl, F.; Perepichka, D. F. Tetrathiafulvalenes, Oligoacenes, and Their Buckminsterfullerene Derivatives: The Brick and Mortar of Organic Electronics. *Chem. Rev.* **2004**, *104*, 4891–4946.
- (8) Anthony, J. E. Functionalized Acenes and Heteroacenes for Organic Electronics. *Chem. Rev.* **2006**, *106*, 5028–5048.
- (9) Kleven, H. B.; Platt, J. R. Spectral Resemblances of Cata-Condensed Hydrocarbons. *J. Chem. Phys.* **1949**, *17*, 470–481.
- (10) Anthony, J. The Larger Acenes: Versatile Organic Semiconductors. *Angew. Chem. Int. Ed.* **2008**, *47*, 452–483.

- (11) Biermann, D.; Schmidt, W. Diels-Alder Reactivity of Polycyclic Aromatic Hydrocarbons. 1. Acenes and Benzologs. *J. Am. Chem. Soc.* **1980**, *102*, 3163–3173.
- (12) Payne, M. M.; Parkin, S. R.; Anthony, J. E. Functionalized Higher Acenes: Hexacene and Heptacene. *J. Am. Chem. Soc.* **2005**, *127*, 8028–8029.
- (13) Mondal, R.; Shah, B. K.; Neckers, D. C. Photogeneration of Heptacene in a Polymer Matrix. *J. Am. Chem. Soc.* **2006**, *128*, 9612–9613.
- (14) Bettinger, H. F.; Mondal, R.; Neckers, D. C. Stable Photoinduced Charge Separation in Heptacene. *Chem. Commun.* **2007**, *48*, 5209–5211.
- (15) Chun, D.; Cheng, Y.; Wudl, F. The Most Stable and Fully Characterized Functionalized Heptacene. *Angew. Chem. Int. Ed.* **2008**, *47*, 8380–8385.
- (16) Mondal, R.; Tönshoff, C.; Khon, D.; Neckers, D. C.; Bettinger, H. F. Synthesis, Stability, and Photochemistry of Pentacene, Hexacene, and Heptacene: A Matrix Isolation Study. *J. Am. Chem. Soc.* **2009**, *131*, 14281–14289.
- (17) Tönshoff, C.; Bettinger, H. Photogeneration of Octacene and Nonacene. *Angew. Chem. Int. Ed.* **2010**, *49*, 4125–4128.
- (18) Kaur, I.; Jazdyk, M.; Stein, N. N.; Prusevich, P.; Miller, G. P. Design, Synthesis, and Characterization of a Persistent Nonacene Derivative. *J. Am. Chem. Soc.* **2010**, *132*, 1261–1263.
- (19) Angliker, H.; Rommel, E.; Wirz, J. Electronic Spectra of Hexacene in Solution (Ground State. Triplet State. Dication and Dianion). *Chem. Phys. Lett.* **1982**, *87*, 208 – 212.
- (20) Houk, K. N.; Lee, P. S.; Nendel, M. Polyacene and Cyclacene Geometries and Electronic Structures: Bond Equalization, Vanishing Band Gaps, and Triplet Ground States Contrast with Polyacetylene. *J. Org. Chem.* **2001**, *66*, 5517–5521.

- (21) Raghu, C.; Anusooya Pati, Y.; Ramasesha, S. Density-Matrix Renormalization-Group Study of Low-Lying Excitations of Polyacene within a Pariser-Parr-Pople Model. *Phys. Rev. B* **2002**, *66*, 035116.
- (22) Gao, Y.; Liu, C.-G.; Jiang, Y.-S. The Valence Bond Study for Benzenoid Hydrocarbons of Medium to Infinite Sizes. *J. Phys. Chem. A* **2002**, *106*, 2592–2597.
- (23) Bendikov, M.; Duong, H. M.; Starkey, K.; Houk, K. N.; Carter, E. A.; Wudl, F. Oligoacenes: Theoretical Prediction of Open-Shell Singlet Diradical Ground States. *J. Am. Chem. Soc.* **2004**, *126*, 7416–7417.
- (24) Hachmann, J.; Dorando, J. J.; Aviles, M.; Chan, G. K.-L. The Radical Character of the Acenes: A Density Matrix Renormalization Group Study. *J. Chem. Phys.* **2007**, *127*, 134309.
- (25) Jiang, D.-en.; Dai, S. Electronic Ground State of Higher Acenes. *J. Phys. Chem. A* **2008**, *112*, 332–335.
- (26) Hajgat6, B.; Huzak, M.; Deleuze, M. S. Focal Point Analysis of the Singlet-Triplet Energy Gap of Octacene and Larger Acenes. *J. Phys. Chem. A* **2011**, *115*, 9282–9293.
- (27) Sony, P.; Shukla, A. Large-Scale Correlated Calculations of Linear Optical Absorption and Low-Lying Excited States of Polyacenes: Pariser-Parr-Pople Hamiltonian. *Phys. Rev. B* **2007**, *75*, 155208.
- (28) Sony, P.; Shukla, A. Large-Scale Correlated Study of Excited State Absorptions in Naphthalene and Anthracene. *J. Chem. Phys.* **2009**, *131*, 014302.
- (29) Raghu, C.; Pati, Y. A.; Ramasesha, S. Structural and Electronic Instabilities in Polyacenes: Density-Matrix Renormalization Group Study of a Long-Range Interacting Model. *Phys. Rev. B* **2002**, *65*, 155204.
- (30) Ohno, K. Some Remarks on the Pariser-Parr-Pople Method. *Theor. Chim. Acta* **1964**, *2*, 219–227.

- (31) Chandross, M.; Mazumdar, S. Coulomb Interactions and Linear, Nonlinear, and Triplet Absorption in Poly(Para-PhenyleneVinylene). *Phys. Rev. B* **1997**, *55*, 1497–1504.
- (32) Sony, P.; Shukla, A. A General Purpose Fortran 90 Electronic Structure Program for Conjugated Systems using Pariser-Parr-Pople Model. *Comput. Phys. Commun.* **2010**, *181*, 821 – 830.
- (33) Buenker, R. J.; Peyerimhoff, S. D.; Butscher, W. Applicability of the Multi-Reference Double-Excitation CI (MRD-CI) Method to the Calculation of Electronic Wavefunctions and Comparison with Related Techniques. *Mol. Phys.* **1978**, *35*, 771–791.
- (34) Buenker, R. J.; Peyerimhoff, S. D. Individualized Configuration Selection in CI Calculations with Subsequent Energy Extrapolation. *Theor. Chim. Acta* **1974**, *35*, 33–58.
- (35) Shukla, A. Correlated Theory of Triplet Photoinduced Absorption in Phenylene-Vinylene Chains. *Phys. Rev. B* **2002**, *65*, 125204.
- (36) Shukla, A. Theory of Nonlinear Optical Properties of Phenyl-Substituted Polyacetylenes. *Phys. Rev. B* **2004**, *69*, 165218.
- (37) Shukla, A. Theory of Two-Photon Absorption in Poly(Diphenyl) Polyacetylenes. *Chem. Phys.* **2004**, *300*, 177 – 188.
- (38) Ghosh, H.; Shukla, A.; Mazumdar, S. Electron-Correlation-Induced Transverse Delocalization and Longitudinal Confinement in Excited States of Phenyl-Substituted Polyacetylenes. *Phys. Rev. B* **2000**, *62*, 12763–12774.
- (39) Mataga, N.; Nishimoto, K. Electronic Structure and Spectra of Some Nitrogen Heterocycles. *Z. Physik. Chemie* **1957**, *12*, 335–338.
- (40) Kiess, H. G.; Baeriswyl, D. *Conjugated Conducting Polymers*; Springer Series in Solid-State Sciences; Springer-Verlag, 1992.

- (41) Salem, L.; Rowland, C. The Electronic Properties of Diradicals. *Angew. Chem. Int. Ed.* **1972**, *11*, 92–111.
- (42) Rayne, S.; Forest, K. Semiempirical, Hartree-Fock, Density Functional, and Second Order Moller-Plesset Perturbation Theory Methods Do Not Accurately Predict Ionization Energies and Electron Affinities of Short- Through Long-Chain [n]Acenes. *Available from Nature Precedings* **2011**, 10.1038/npre.2011.6578.1.

Graphical TOC Entry

